



# Quantifying microbial metabolism in soils using calorimetry — A bioenergetics perspective

Arjun Chakrawal<sup>a,b,\*</sup>, Anke M. Herrmann<sup>c</sup>, Hana Šantrůčková<sup>d</sup>, Stefano Manzoni<sup>a,b</sup>

<sup>a</sup> Department of Physical Geography, Stockholm University, Svante Arrhenius väg 8C, Frescati, SE-10691, Stockholm, Sweden

<sup>b</sup> Bolin Centre for Climate Research, Stockholm University, Stockholm, Sweden

<sup>c</sup> Department of Soil & Environment, Swedish University of Agricultural Sciences, P.O. Box 7014, 75007, Uppsala, Sweden

<sup>d</sup> Department of Ecosystem Biology, University of South Bohemia, České Budějovice, Czech Republic

## ARTICLE INFO

### Keywords:

Bioenergetics  
Microbial growth  
Calorespirometric ratio  
Carbon-use efficiency  
Priming effect  
Glucose metabolism

## ABSTRACT

Microbial carbon use efficiency (CUE) measures the partitioning between anabolic and catabolic processes. While most work on CUE has been based on carbon (C) mass flows, the roles of organic C energy contents and microbial energy demand on CUE have been rarely considered. Thus, a bioenergetics perspective could provide new insights on how microorganisms utilize C and ultimately allow evaluating their role in C stabilization in soils. Recently, the calorespirometric ratio (CR)—the ratio of heat dissipation and respiration—has been used to characterize the efficiency of microbial growth in soils. Here, we formulate a coupled mass and energy balance model for microbial growth and provide a generalized relationship between CUE and CR. In the model, we consider two types of organic C in soils: an added substrate (e.g., glucose) and the native soil organic matter (SOM), to also account for priming effects. Furthermore, we consider both aerobic and fermentation metabolic pathways. We use this model as a framework to generalize previous formulations and generate hypotheses on the expected variations in CR as a function of substrate quality, metabolic pathways, and microbial traits (specifically CUE). In turn, the same equations can be used to estimate CUE from measured CR.

Our results confirm previous findings on CR and show that without microbial growth, CR depends only on the rates of the different metabolic pathways, while CR is also a function of the growth yields for these metabolic pathways when microbial growth occurs. Under strictly aerobic conditions, CUE increases with increasing CR for substrates with a higher degree of reduction than that of the microbial biomass, while CUE decreases with increasing CR for substrates with a lower degree of reduction than the microbial biomass. When aerobic reactions and fermentation occur simultaneously, the relation between CUE and CR is mediated by (i) the degree of reduction of the substrates, (ii) the rates and growth yields of all metabolic pathways, and (iii) the contribution of SOM priming to microbial growth. Using the proposed framework, calorimetry can be used to evaluate CUE and the role of different metabolic pathways in soil systems.

## 1. Introduction

Soil organic matter (SOM) provides both energy (catabolism) and materials for biosynthesis (anabolism) to soil microorganisms. The partitioning of C between these two processes affects the ultimate fate of C—either removed from the soil as CO<sub>2</sub> or retained and stabilized in SOM. Microbial carbon use efficiency (CUE)—the ratio of C used for biosynthesis over C consumed—measures how much of the C used by microbes is routed to anabolic reactions, and thus remains in the soil (Cotrufo et al., 2013; Manzoni et al., 2018). This efficiency concept is not new, as its origin can be traced back to studies on microbial growth in the late 1940s (Monod, 1949). However, only recently and

thanks to methodological advances, CUE has become a frequently measured parameter in soil C cycling studies. CUE varies across spatial scales from microbial cell to ecosystem scale (Geyer et al., 2016; Manzoni et al., 2018) and is affected by soil physio-chemical environment, climatic conditions, and soil microbial community composition and their activity (Manzoni et al., 2012; Bölscher et al., 2020). Because the drivers and variability of CUE are still not fully understood, finding methods to quantify CUE reliably across systems and experimental setups is particularly important.

While most work on C cycling has focused on CUE in terms of C mass flows through microbial biomass, the partitioning of C to anabolic

\* Corresponding author at: Department of Physical Geography, Stockholm University, Svante Arrhenius väg 8C, Frescati, SE-10691, Stockholm, Sweden.

E-mail addresses: [arjun.chakrawal@natgeo.su.se](mailto:arjun.chakrawal@natgeo.su.se) (A. Chakrawal), [Anke.Herrmann@slu.se](mailto:Anke.Herrmann@slu.se) (A.M. Herrmann), [hana.santruckova@prf.jcu.cz](mailto:hana.santruckova@prf.jcu.cz) (H. Šantrůčková), [stefano.manzoni@natgeo.su.se](mailto:stefano.manzoni@natgeo.su.se) (S. Manzoni).

<https://doi.org/10.1016/j.soilbio.2020.107945>

Received 16 May 2020; Received in revised form 19 July 2020; Accepted 29 July 2020

Available online 3 August 2020

0038-0717/© 2020 The Authors. Published by Elsevier Ltd. This is an open access article under the CC BY license (<http://creativecommons.org/licenses/by/4.0/>).

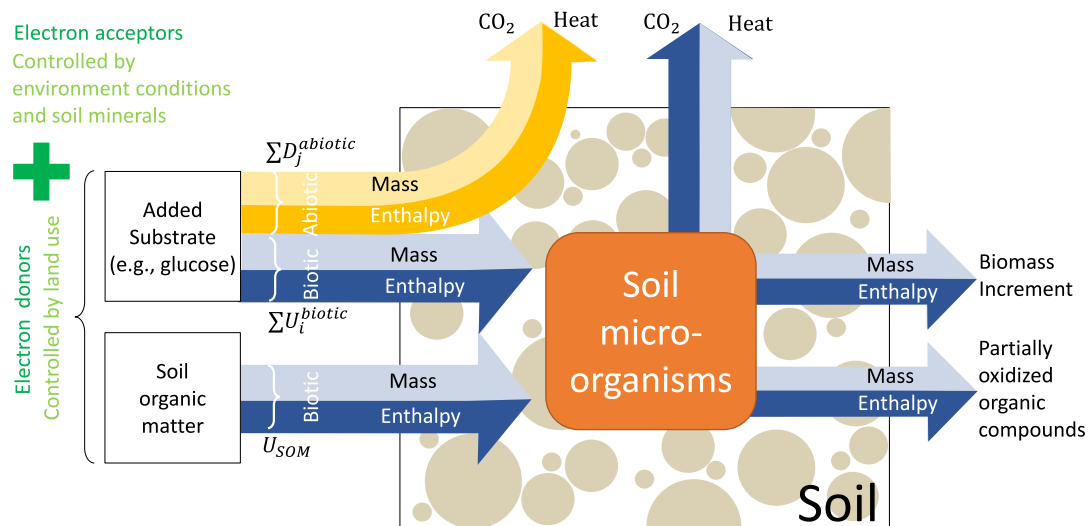


**Fig. 1.** Schematic of mass and energy flows: The interactions of substrate and SOM with soil matrix (abiotic) and microorganisms (biotic) are mass and energy dissipation processes that result in the production of CO<sub>2</sub> and heat. Abiotic processes are the reactions of organic C with soil minerals, and the biotic processes are the microbial growth reactions. Microbial growth reactions are redox reactions in which organic C generally acts as electron donors and the source of C, and the inorganic compounds (such as O<sub>2</sub>, NO<sub>3</sub><sup>-</sup>, SO<sub>4</sub><sup>2-</sup> etc.) as electron acceptors. In this work, two sources of organic C are considered: an added substrate (e.g., glucose) and native soil organic matter C. Both biotic (at rate  $\Sigma U_i^{biotic}$ ) and abiotic processes (at rate  $\Sigma D_j^{abiotic}$ ) are considered for the degradation of the added substrate, whereas only biotic processes are considered for the native SOM ( $U_{SOM}$ ). If the abiotic processes are endothermic reactions, then the yellow arrows would be directed towards the system.

and catabolic pathways (and thus CUE) can only be understood by considering the coupled C mass and energy flows (Roels, 1980a; Gommers et al., 1988; Minkevich and Eroshin, 1973). Microorganisms that feed on low energy (more oxidized) substrates are energy limited; therefore, they cannot have high CUE and release more C per unit substrate than C-limited microbes that feed on high energy (more reduced) substrates. Thus, a bioenergetics perspective on CUE could leverage the additional information that heat exchanges provide by combining C and heat exchange measurements. This approach is referred to as calorimetry (Hansen et al., 2004).

Over the past two decades, measurements of heat produced during organic matter decomposition have been increasingly used to quantify microbial activity in soils; however, the application of these methods is still in its early stage (Barros et al., 2016b; Arnoldt-Schmitt et al., 2016; Arnoldt-Schmitt, 2017; Geyer et al., 2019; Colombi et al., 2019; Maskow et al., 2019). One of the earliest examples of using heat as a proxy for microbial activity was to assess the effect of pH and substrate addition on heat dissipated in soils (Ljungholm et al., 1979). Since then, calorimetry has emerged as a useful tool in soil science because of its nondestructive measurement capabilities (Barja and Núñez, 1999; Barros et al., 2011; Chaires et al., 2015; Herrmann and Bölscher, 2015; Bölscher et al., 2017; Herrmann and Colombi, 2019). While C fluxes provide information only on decomposition rates, calorimetry—by combining heat production and respiration rates—can provide insights into the chemical nature of substrates and the metabolic pathways supplying microbial growth (Hansen et al., 2004). Several authors have shown the potential of using the ratio of heat production rate and respiration rate to characterize the oxidative state of organic compounds and microbial growth yield (Roels, 1980a; von Stockar and Marison, 1989; Hansen et al., 2004). This ratio is referred to as calorimetric ratio (CR). The CR is typically expressed in kJ C-mol<sup>-1</sup> CO<sub>2</sub> when the heat production rate is in kJ g<sup>-1</sup> soil h<sup>-1</sup> and the CO<sub>2</sub> production rate is in C-mol CO<sub>2</sub> g<sup>-1</sup> soil h<sup>-1</sup>. In soils, Sparling (1983) was the first to report the observed value of the CR and relate it to microbial growth. Building on these applications, CR can be used to estimate CUE (Hansen et al., 2004). Recently, Geyer et al. (2019) compared CUE estimates from CR to those from other methods, showing that the CR-based method can be useful only when considering multiple metabolic pathways in the calculations, which is rarely done.

In this article, we explore the potential of calorimetry to evaluate soil microbial metabolism on simple substrates and SOM via priming. Several approaches from the biotechnology and thermodynamics literature have been proposed to relate carbon and heat fluxes associated with microbial processes (Minkevich and Eroshin, 1973; Nagai, 1979; Roels, 1980a; Birou et al., 1987; von Stockar and Birou, 1989; Gnaiger and Kemp, 1990; von Stockar and Liu, 1999; Matheson et al., 2004; Kleerebezem and Van Loosdrecht, 2010; Battley, 2013). However, a comprehensive synthesis relevant to soil science, including both metabolism on simple substrates and SOM via priming, is missing and motivates the development of a general theoretical framework for soil bioenergetics.

The heat and CO<sub>2</sub> production rates measured in calorimetric experiments are the average responses of a multitude of metabolic reactions; e.g., aerobic and anaerobic respiration, fermentation, and biosynthesis. This makes interpretation of CR data challenging. Currently, models used to link CUE and CR are mostly based on aerobic conditions (Maskow and Paufler, 2015; Wadsö and Hansen, 2015; Hansen et al., 2004), hence these approaches have limited applicability (Geyer et al., 2019). Under aerobic conditions and in non-growing systems, a theoretical value of CR can be calculated using the degree of reduction (DR) of the organic carbon and Thornton's constant (heat production per unit of consumed O<sub>2</sub> (Hansen et al., 2004)). For example, during complete oxidation of glucose to CO<sub>2</sub>, CR is equal to 469 kJ C-mol<sup>-1</sup> CO<sub>2</sub>, which is equivalent to the enthalpy of combustion of glucose. Hansen et al. (2004) also provided a relationship between the CR and the biomass yield of soil microorganisms in aerobic growth conditions. The assumption of aerobic growth fails to address the large differences among observed CR values from soils (Herrmann and Bölscher, 2015). In soil systems, these deviations have been generally associated with metabolic processes contributing to heat or CO<sub>2</sub> production other than aerobic growth, such as anaerobic respiration and fermentation pathways (Sparling, 1983; Boye et al., 2018). However, these fermentation pathways have not been explicitly included in a theoretical framework including both mass and energy flows.

Furthermore, growth on the high-quality substrates typically used in calorimetry may induce the mineralization of low quality substrates (such as SOM)—the so-called priming effect. SOM priming contributes to microbial growth thereby affecting CUE and heat exchanges (Arcand et al., 2017). Therefore, calorimetry could be

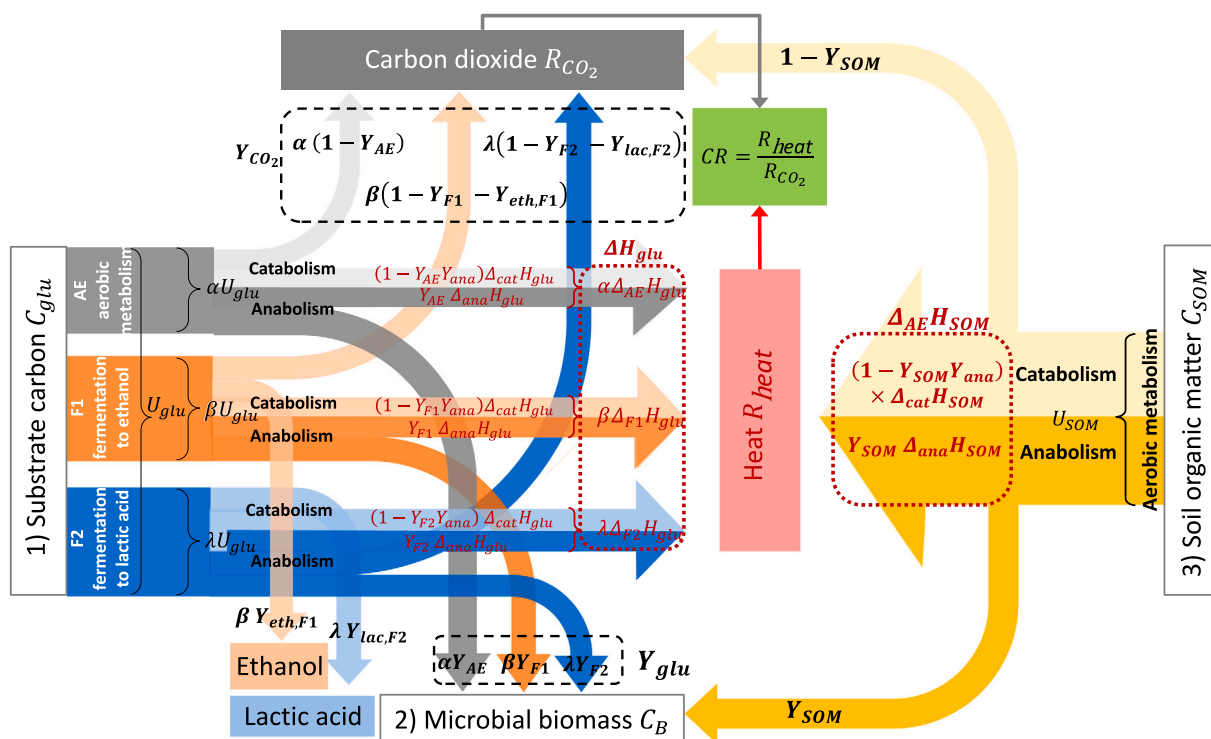


**Fig. 2.** Energetic model framework including three C pools: (1) added substrate (glucose,  $C_{glu}$ ), (2) microbial biomass ( $C_B$ ), and (3) native soil organic C ( $C_{SOM}$ ). Glucose is taken up via three metabolic pathways i.e. aerobic (AE), fermentation to ethanol (F1) and fermentation to lactic acid (F2). For simplicity, we chose only aerobic metabolism of SOM.  $U_{glu}$  and  $U_{SOM}$  are the total uptake rates of glucose and SOM, respectively.  $\alpha$ ,  $\beta$  and  $\lambda$  are the fractions of  $U_{glu}$  routed to AE, F1 and F2, respectively. The microbial growth reaction is divided into its catabolic and anabolic components. Catabolism in AE and F1 metabolism produces  $CO_2$  and byproducts (ethanol in F1), but in F2,  $CO_2$  is also produced from anabolism (see Appendix A for details).  $Y_{AE}$ ,  $Y_{F1}$  and  $Y_{F2}$  are the biomass yields of AE, F1 and F2, respectively, so that the overall biomass yield on glucose is given by  $Y_{glu} = \alpha Y_{AE} + \beta Y_{F1} + \lambda Y_{F2}$ . Similarly, overall  $CO_2$  yield is  $Y_{CO_2} = \alpha(1 - Y_{AE}) + \beta(1 - Y_{F1} - Y_{eth,F1}) + \lambda(1 - Y_{F2} - Y_{lac,F2})$ , where  $Y_{eth,F1}$  and  $Y_{lac,F2}$  are the yields of ethanol and lactic acid in F1 and F2, respectively. The amount of heat released from each metabolic pathway is calculated by adding the changes in enthalpies of catabolism and anabolism.  $\Delta_{AE}H_{glu}$ ,  $\Delta_{F1}H_{glu}$  and  $\Delta_{F2}H_{glu}$  are respectively the enthalpies of reaction of AE, F1 and F2, resulting in a total heat released per C-mol of glucose metabolized of  $\Delta H_{glu} = \alpha \Delta_{AE}H_{glu} + \beta \Delta_{F1}H_{glu} + \lambda \Delta_{F2}H_{glu}$ .  $R_{heat}$  and  $R_{CO_2}$  are the total heat and  $CO_2$  production rates and their ratio is the calorespirometric ratio (CR).

used to quantify the priming effect (Bölscher et al., 2017), as an alternative to the typical mass balance approaches using stable isotope tracers (Kuzyakov, 2010; Wutzler and Reichstein, 2013; Arcand et al., 2017). As for the fermentation pathways, also priming effects have not been integrated into a coherent bioenergetic framework for soils.

Here, we present such a framework to link microbial traits and metabolism to the heat and  $CO_2$  production rates, and the calorespirometric ratio. We consider two sources of organic C (Fig. 1): an added substrate (using glucose as an example) and SOM, which is important to study priming effects. For the example of growth on glucose, we consider aerobic and two common fermentation pathways differing in end products and  $CO_2$  release (Fig. 2). The proposed theoretical framework is used to answer the following questions:

1. Can a simple aerobic/fermentation energetics model assist in the interpretation of CR data? (Section 2)
2. How do different catabolic processes and their rates affect CR (e.g., varying degrees of aerobicity and fermentation)? (Section 3.1)
3. Can CR be used to estimate CUE? (Section 3.2)
4. How is priming affecting the CUE–CR relation? (Section 3.2.2)
5. How does CR vary when different types of organic compounds are decomposed? (Section 4)

## 2. A general mass-energy model for microbial metabolism in soils

We start by presenting a general mass-energy balance model that describes microbial metabolism under a range of growth conditions (Fig. 1). This model is used to interpret measured calorespirometric ratios. Calorespirometric experiments are often performed in a substrate

induced environment that stimulates the microbial activity. The energy dissipated in catabolism as heat and C fluxes released as  $CO_2$  from the soils are measured as responses against the control in which the substrate is not added. This heat and/or  $CO_2$  produced are the average response of a multitude of metabolic reactions that may be exergonic or endergonic and may or may not produce  $CO_2$ . Moreover, the introduction of a substrate may induce priming, which can contribute additional heat and  $CO_2$  as a result of the decomposition of SOM (Kuzyakov, 2010). By taking into account mass and energy flows from the uptake and metabolism of the added substrate and native SOM, we build an energetics model framework that links CR to aerobic and fermentation metabolic rates and CUE.

In all analyses presented in the following sections, we assume standard temperature, pressure, and pH=7. The processes involved (and the corresponding symbolic representations) are illustrated in Fig. 2, and all symbols and their units are defined in Table 1.

### 2.1. Mass balances for substrates and microbial biomass

The mass balances are set up based on the schematic in Fig. 1, which refers to the specific case of glucose (subscript  $glu$ ) as a substrate (generic subscript  $S$ ). We consider three pools of carbon: (1) added substrate ( $C_S$ ), (2) microbial biomass ( $C_B$ , generic subscript  $B$  for biomass), and (3) SOM ( $C_{SOM}$ ). Added substrates such as glucose can be easily taken up by a range of microorganisms (at a rate  $U_i^{Biotic}$ ), but they can also undergo abiotic mineralization ( $D_j^{Abiotic}$ ). We differentiate biotic processes (the degradation of substrate mediated by microorganisms) from abiotic processes that result from the interaction of substrates with soil minerals, such as sorption/adsorption reactions. SOM is taken up at a rate  $U_{SOM}$ , which is much slower compared to

**Table 1**  
List of symbols and acronyms (subscript symbols and acronyms are listed as footnote).

Symbol	Description	Unit
$\alpha$	Fraction of the overall uptake rate of glucose via aerobic pathway	dimensionless
$\beta$	Fraction of the overall uptake rate of glucose via F1 pathway	dimensionless
$\lambda$	Fraction of the overall uptake rate of glucose via F2 pathway	dimensionless
$\Delta H_{glu}$	Overall enthalpy change of glucose metabolism	kJ C-mol <sup>-1</sup> glu
$\Delta_{ana} H_B$	Enthalpy change of anabolism	kJ C-mol <sup>-1</sup> B
$\Delta_{cat,i} H_{glu}$	Enthalpy change of catabolism of glucose (with $i = AE, F1,$ and $F2$ )	kJ C-mol <sup>-1</sup> glu
$\Delta_i H_{glu}$	Enthalpy of growth reaction on glucose (with $i = AE, F1,$ and $F2$ )	kJ C-mol <sup>-1</sup> glu
$\Delta_{AE} H_{SOM}$	Enthalpy of growth reaction on SOM under aerobic conditions	kJ C-mol <sup>-1</sup> SOM
$\Delta H_T$	Thornton's constant (−469 for glucose, −455 for other organic compounds)	kJ mol <sup>-1</sup> O <sub>2</sub>
$\gamma_B$	Degree of reduction of biomass	e <sup>−</sup> mol C-mol <sup>-1</sup> B
$\gamma_{glu}$	Degree of reduction of glucose	e <sup>−</sup> mol C-mol <sup>-1</sup> glu
$\gamma_S$	Degree of reduction of generic substrate	e <sup>−</sup> mol C-mol <sup>-1</sup> S
$C_B$	Microbial biomass C	C-mol g <sup>-1</sup> soil
CR	Calorespirometric ratio	kJ C-mol <sup>-1</sup> CO <sub>2</sub>
$C_S$	Substrate C	C-mol g <sup>-1</sup> soil
$C_{SOM}$	Soil organic matter C	C-mol g <sup>-1</sup> soil
CUE	Carbon use efficiency	C-mol B C-mol <sup>-1</sup> S
$D_j^{Abiotic}$	Rate of degradation of substrate for $j$ th via abiotic chemical reaction	C-mol S g <sup>-1</sup> soil h <sup>-1</sup>
DR	Degree of reduction	
NOSC	Nominal oxidation state of C	
$Q$	Rate of heat production from all the biotic and abiotic reactions	kJ g <sup>-1</sup> soil h <sup>-1</sup>
$r_p$	Ratio of the rates of uptake of glucose and SOM	dimensionless
$U_i^{Biotic}$	Uptake rate of glucose for $i$ th biotic metabolic reaction	C-mol glu g <sup>-1</sup> soil h <sup>-1</sup>
$U_{glu}$	Overall uptake rate of glucose	C-mol glu g <sup>-1</sup> soil h <sup>-1</sup>
$U_{SOM}$	Uptake rate of SOM under aerobic conditions	C-mol SOM g <sup>-1</sup> soil h <sup>-1</sup>
$Y_{ana}$	Stoichiometry of substrate in anabolic reaction	C-mol B C-mol <sup>-1</sup> S
$Y_{AE}$	Aerobic microbial growth yield for glucose	C-mol B C-mol <sup>-1</sup> glu
$Y_{CO_2}$	Overall CO <sub>2</sub> yield from glucose metabolism	C-mol CO <sub>2</sub> C-mol <sup>-1</sup> glu
$Y_{C,i}$	CO <sub>2</sub> yield from $i$ glucose metabolism (with $i = AE, F1,$ and $F2$ )	C-mol CO <sub>2</sub> C-mol <sup>-1</sup> glu
$Y_{C,SOM}$	CO <sub>2</sub> yield from SOM metabolism	C-mol CO <sub>2</sub> C-mol <sup>-1</sup> SOM
$Y_{glu}$	Carbon use efficiency for microbial growth on glucose	C-mol B C-mol <sup>-1</sup> glu
$Y_{eth,F1}$	Ethanol yield in fermentation F1 pathway	C-mol eth C-mol <sup>-1</sup> glu
$Y_{F1}$	Microbial growth yield in fermentation F1 pathway	C-mol B C-mol <sup>-1</sup> glu
$Y_{F2}$	Microbial growth yield in fermentation F2 pathway	C-mol B C-mol <sup>-1</sup> glu
$Y_{i,glu}^{max}$	Maximum microbial yield of glucose for different metabolic pathways (with $i = AE, F1,$ and $F2$ )	C-mol B C-mol <sup>-1</sup> glu
$Y_{AE,S}^{max}$	maximum microbial yield of generic substrate (S) for aerobic pathway	C-mol B C-mol <sup>-1</sup> S
$Y_{lac,F2}$	Lactic acid yield in fermentation F2 pathway	C-mol lac C-mol <sup>-1</sup> glu
$Y_{SOM}$	Aerobic microbial growth yield for SOM	C-mol B C-mol <sup>-1</sup> SOM

AE: aerobic, ana: anabolism, B: biomass, cat: catabolism, eth: ethanol, F1: fermentation of glucose to ethanol, F2: fermentation of glucose to lactic acid, glu: glucose, lac:lactic acid, S: substrate, and SOM: native soil organic matter.

that of the added substrate (mineralization time scales of SOM are in the order of months to decades, while those of glucose are in the order of hours). For simplicity, we consider only biotic degradation of SOM under completely aerobic conditions; thus,  $U_{SOM}$  represents the biotic uptake rate of SOM.

Microorganisms are assumed to grow on both  $C_S$  and  $C_{SOM}$ , but with different growth yields. Often calorimetric experiments last for a few hours to days (Barros Pena, 2018), so that mortality and recycling of dead microorganisms, which have longer turnover time (Spohn et al., 2016), can be neglected in the microbial C balance. The mass balance equations for the three C pools are written in terms of C moles; e.g., glucose (C<sub>6</sub>H<sub>12</sub>O<sub>6</sub>) is written as CH<sub>2</sub>O (1 C-mol glucose), and microbial biomass is written as CH<sub>1.8</sub>O<sub>0.5</sub>N<sub>0.2</sub> (1 C-mol biomass) (Roels, 1980a). Thus, all C rates have units of C-mol substrate or SOM g<sup>-1</sup> soil h<sup>-1</sup> and growth yields are expressed in C-mol biomass C-mol<sup>-1</sup> of substrate or SOM. The mass balance equations for the three C pools and CO<sub>2</sub> can be written as (see Fig. 1),

$$\frac{dC_S}{dt} = - \sum_i U_i^{Biotic} - \sum_j D_j^{Abiotic}, \quad (1)$$

$$\frac{dC_B}{dt} = \sum_i Y_i U_i^{Biotic} + Y_{SOM} U_{SOM}, \quad (2)$$

$$\frac{dC_{SOM}}{dt} = -U_{SOM}, \quad (3)$$

$$\frac{dCO_2}{dt} = \sum_i Y_{C,i} U_i^{Biotic} + \sum_j D_j^{Abiotic} + Y_{C,SOM} U_{SOM}. \quad (4)$$

where  $C_S$ ,  $C_B$  and  $C_{SOM}$  are respectively the added substrate C (thereafter referred to as substrate), microbial C and SOM.  $U_i^{Biotic}$  is the

uptake rate of added substrate via biotic pathways, and  $i$  refers to various pathways (aerobic, anaerobic and fermentation); and  $Y_i$  and  $Y_{C,i}$  represent the biomass and CO<sub>2</sub> yields for that pathway.  $D_j^{Abiotic}$  is the degradation rate of the added substrate via abiotic pathways, and  $j$  refers to various abiotic pathways. The rate of uptake of SOM is denoted by  $U_{SOM}$  and the corresponding biomass and CO<sub>2</sub> yields by  $Y_{SOM}$  and  $Y_{C,SOM}$ , respectively.

Carbon use efficiency is defined as the microbial growth rate divided by the total C uptake rate (Manzoni et al., 2012). Because the microbial growth rate (Eq. (2)) is supported by two C sources (added substrate and SOM; Eqs. (1) and (3)), a general expression of CUE is given by

$$CUE = \frac{\sum_i Y_i U_i^{Biotic} + Y_{SOM} U_{SOM}}{\sum_i U_i^{Biotic} + U_{SOM}}. \quad (5)$$

We will return to CUE in Section 3, where the relationship between CUE and CR is determined.

## 2.2. Energy balance for the soil system

In an isothermal system with constant volume and no external inputs of heat or matter, the only source of heat is from the chemical reactions taking place inside the system (von Stockar and van der Wie- len, 2013). Thus, the rate of heat production is given by the enthalpy of the reaction multiplied by the rate of the reaction. The overall soil

heat production rate  $Q$  in  $\text{kJ g}^{-1} \text{ soil h}^{-1}$  is the sum of the rates of heat produced from the individual metabolic reactions (Fig. 1),

$$Q = - \left( \sum_i \Delta_i H_S^{\text{Biotic}} U_i^{\text{Biotic}} + \sum_j \Delta_j H_S^{\text{Abiotic}} D_j^{\text{Abiotic}} + \Delta_{AE} H_{SOM} U_{SOM} \right), \quad (6)$$

where  $\Delta_i H_S^{\text{Biotic}}$  and  $\Delta_j H_S^{\text{Abiotic}}$  are the enthalpies of reaction of substrate uptake and degradation via biotic and abiotic pathways, respectively; and  $\Delta H_{SOM}$  is the enthalpy of reaction of SOM uptake and metabolism. The negative sign accounts for the negative values of the reaction enthalpies. Note that the first subscript,  $i$ , refers to the metabolic reaction and the second subscript,  $S$  or  $SOM$ , refers to the compound with respect to which the enthalpy of the reaction is calculated. For example,  $\Delta_i H_S$  indicates the enthalpy change for substrate  $S$  along the metabolic pathway  $i$ , and is expressed in  $\text{kJ C-mol}^{-1}$  of substrate. This notation has been used throughout the text.

### 2.3. Definition of calorespirometric ratio

Based on these mass and energy balance equations, we can now define the CR as the ratio of heat production rate (Eq. (6)) to  $\text{CO}_2$  production rate (Eq. (4)) as follows,

$$CR = - \frac{\sum_i \Delta_i H_S^{\text{Biotic}} U_i^{\text{Biotic}} + \sum_j \Delta_j H_S^{\text{Abiotic}} D_j^{\text{Abiotic}} + \Delta_{AE} H_{SOM} U_{SOM}}{\sum_i Y_{C,i} U_i^{\text{Biotic}} + \sum_j D_j^{\text{Abiotic}} + Y_{C,SOM} U_{SOM}}. \quad (7)$$

This general equation links CR to the rates of individual processes and the associated enthalpy changes. As such, it provides the theoretical foundation to answer our first question on using a bioenergetics model to interpret patterns in CR. To apply Eq. (7), first, the biotic processes occurring are specified, and then the equation is re-written for convenience in terms of normalized reaction rates. The biotic processes for the added substrates are grouped according to different metabolic pathways: aerobic and two fermentation pathways (Fig. 2). We have considered the example of glucose as the added substrate (subscript  $S = glu$ ), even though the same rationale can be adapted to other substrates as well. To keep the theory tractable, we focus on two fermentation pathways: ethanol fermentation (F1) and lactic acid (homolactic) fermentation (F2). These two fermentation pathways were chosen because they uniquely describe the role of  $\text{CO}_2$  in fermentative metabolism of glucose. During ethanol fermentation, catabolism of 1 C-mole of glucose produces in two-third C-mole of ethanol and one-third C-mole of  $\text{CO}_2$ , while catabolism of 1-C mole of glucose in lactic acid fermentation only produces 1-C mole of lactic acid. The chemical reactions for the metabolism of glucose following each pathway are described in Appendix A as Eqs. (A.4), (A.5), and (A.6) for aerobic, fermentation F1, and F2 pathways, respectively.

Since the interactions of typical added substrates (e.g., glucose) with soil minerals produces a negligible amount of heat and  $\text{CO}_2$  (Hermmann et al., 2014), abiotic reactions are not included in the following; i.e.,  $D_i^{\text{Abiotic}} = 0$ . For the biotic uptake of SOM, we consider only the aerobic metabolic pathway; thus,  $\Delta_{AE} H_{SOM}$  represents the enthalpy of metabolic reaction on SOM under aerobic growth conditions.

To normalize the reaction rates,  $\alpha$ ,  $\beta$  and  $\lambda$  are defined as the fractions of the overall substrate uptake rate ( $\sum_i U_i^{\text{Biotic}}$ ); i.e.,  $\alpha = \frac{U_{AE}}{\sum_i U_i^{\text{Biotic}}}$ ,  $\beta = \frac{U_{F1}}{\sum_i U_i^{\text{Biotic}}}$ , and  $\lambda = \frac{U_{F2}}{\sum_i U_i^{\text{Biotic}}}$ . The sum of the fractional rates  $\alpha$ ,  $\beta$  and  $\lambda$  is unity by definition. The parameter  $\alpha$  is also referred to as degree of 'aerobicity' in mixed metabolism (von Stockar and Birou, 1989). When  $\alpha = 1$ , glucose is taken up completely via the aerobic pathway, whereas metabolism is completely fermentative if  $\alpha = 0$ . The fractional rates  $\beta$  and  $\lambda$  can be considered as degrees of fermentation. We also define  $r_p$  as the ratio of  $U_{SOM}$  and the overall substrate uptake

rate, as a measure of priming. The equation for CR is accordingly simplified as,

$$CR = - \frac{\alpha \Delta_{AE} H_S + \beta \Delta_{F1} H_S + \lambda \Delta_{F2} H_S + r_p \Delta_{AE} H_{SOM}}{\alpha Y_{C,AE} + \beta Y_{C,F1} + \lambda Y_{C,F2} + r_p Y_{C,SOM}}. \quad (8)$$

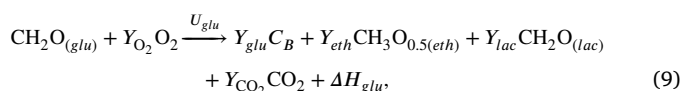
In Eq. (8), the first three terms of the numerator represent the heat production rate from substrate metabolism, and the fourth term represents the heat production rate from SOM metabolism. Similarly, in the denominator, the first three terms represent the total rate of  $\text{CO}_2$  production from substrate metabolism, and the fourth term is the rate of  $\text{CO}_2$  production from SOM metabolism. The choice of the fractional rates allows analyzing the role of different metabolic pathways on CR, as illustrated in Section 3.1 for simple case studies.

Eq. (8) links CR to changes in enthalpy along the various metabolic pathways. In turn, these changes in enthalpy are functions of the microbial growth efficiencies for those pathways, thereby establishing an implicit relation between CR and growth yields (and ultimately CUE). To proceed and make this relation explicit, changes in enthalpy must be related to the corresponding yields, as described in the following section.

### 2.4. Linking the change in enthalpy for microbial growth reactions to growth efficiencies

Changes in enthalpy in Eq. (8) are calculated based on the microbial growth equation for each metabolic pathway. The growth equation can be written as the sum of catabolic and anabolic reactions (von Stockar et al., 2008; Battley, 2009; Smeaton and Van Cappellen, 2018). Catabolic reactions are either complete oxidation (under aerobic conditions) or partial oxidation of the substrate (under anaerobic conditions) that dissipates Gibbs energy, which in turn drives the anabolic reactions (Table A.1). Among the three alternative ways for writing anabolic reactions (Table A.2), we selected the electron balance approach by Battley (2009). If the substrate is more oxidized than the biomass (e.g., glucose), then  $\text{CO}_2$  is released. In contrast, if the substrate is less oxidized (e.g., ethanol), then  $\text{CO}_2$  is utilized in anabolism. We also assume that in the fermentation pathways, products other than biomass are produced only through catabolism. Detailed procedures for writing the catabolic, anabolic, and growth reactions for each pathway can be found in Appendix A.

The overall microbial growth reaction on glucose can be written as Eq. (9). Note that the following equation is only a black-box (macrochemical) representation of glucose uptake—not the actual biochemical metabolic reaction. This is also true for the actual catabolic and anabolic reactions for each pathway in Appendix A.



where  $Y_{\text{O}_2}$ ,  $Y_{glu}$ ,  $Y_{eth}$ ,  $Y_{lac}$  and  $Y_{\text{CO}_2}$  are the stoichiometric coefficients of oxygen, biomass, ethanol, lactic acid and  $\text{CO}_2$  on glucose, respectively.  $\Delta H_{glu}$  is the overall enthalpy of the above reaction; i.e., heat in  $\text{kJ}$  generated per C-mol of glucose metabolized. These stoichiometric coefficients can be written as a function of the fractional rates that partition the overall glucose uptake rate ( $U_{glu}$ ) among the different metabolic pathways (i.e.,  $\alpha$ ,  $\beta$  and  $\lambda$ ), and the respective biomass growth yields (i.e.,  $Y_{AE}$ ,  $Y_{F1}$  and  $Y_{F2}$ ; see Fig. 2),

$$Y_{\text{O}_2} = \alpha \left( \frac{Y_{glu} - Y_{AE} \gamma_B}{4} \right), \quad (10)$$

$$Y_{glu} = \alpha Y_{AE} + \beta Y_{F1} + \lambda Y_{F2}, \quad (11)$$

$$Y_{eth} = \beta Y_{eth,F1} = \beta \left( \frac{Y_{glu} - Y_{F1} \gamma_B}{\gamma_{eth}} \right), \quad (12)$$

$$Y_{lac} = \lambda Y_{lac,F2} = \lambda \left( \frac{Y_{glu} - Y_{F2} \gamma_B}{\gamma_{lac}} \right), \quad (13)$$

$$Y_{\text{CO}_2} = \alpha Y_{C,AE} + \beta Y_{C,F1} + \lambda Y_{C,F2}, \quad (14)$$

**Table 2**Thermodynamic properties of selected organic compounds; CO<sub>2</sub>, NH<sub>3</sub>, H<sub>2</sub>O are used as reference compounds with zero degree of reduction.

Substrate (1 C-mol)	DR <sup>a</sup> (e <sup>-</sup> mol C-mol <sup>-1</sup> )	NOSC <sup>b</sup>	Enthalpy of combustion (kJ C-mol <sup>-1</sup> ) for aerobic reactions = $\frac{DR}{4} \Delta H_T$
glucose CH <sub>2</sub> O( <i>glu</i> )	4	0	-469
lactic acid CH <sub>2</sub> O( <i>lac</i> )	4	0	-469
ethanol CH <sub>3</sub> O <sub>0.5</sub>	6	-2	-703.5
acetic acid CH <sub>2</sub> O( <i>ace</i> )	4	0	-469
oxalic acid CHO <sub>2</sub>	1	3	-117.3
formic acid CH <sub>2</sub> O <sub>2</sub>	2	2	-234.5
biomass CH <sub>1.8</sub> O <sub>0.5</sub> N <sub>0.2</sub>	4.2 or 4.32 <sup>c</sup>	-0.2 or -0.32	-492.5

<sup>a</sup>Degree of reduction,  $DR = 4C + H - 2O - 3N = (4 - NOSC)C$ <sup>b</sup>Nominal oxidation state of C,  $NOSC = 4 - \frac{4C+H-2O-3N}{C} = 4 - \frac{DR}{C}$ ; where C, H, O, and N are the number of carbon, hydrogen, nitrogen, and oxygen atoms in 1 mole of substrate.<sup>c</sup>The DR of biomass is 4.2 and 4.32 are when  $\Delta H_T$  is -469 and -455 kJ mol<sup>-1</sup> O<sub>2</sub>, respectively.

$$\Delta H_{glu} = \alpha \Delta_{AE} H_{glu} + \beta \Delta_{F1} H_{glu} + \lambda \Delta_{F2} H_{glu}, \quad (15)$$

where  $Y_{eth,F1}$  and  $Y_{lac,F2}$  are the product yields of ethanol and lactic acid in metabolic pathways F1 and F2, respectively (Eqs. (A.7) and (A.8));  $\gamma_{glu}$ ,  $\gamma_B$ ,  $\gamma_{eth}$  and  $\gamma_{lac}$  are the degrees of reduction of glucose, biomass, ethanol and lactic acid (Table 2);  $\Delta_{AE} H_{glu}$ ,  $\Delta_{F1} H_{glu}$  and  $\Delta_{F2} H_{glu}$  are the enthalpy changes of the microbial growth reactions for each metabolic pathway.  $Y_{CO_2}$  represents the overall yield of CO<sub>2</sub>, which is a rate weighted yields of CO<sub>2</sub> from each metabolic pathway, and given as follows,

$$Y_{C,AE} = 1 - Y_{AE}, \quad (16)$$

$$Y_{C,F1} = 1 - Y_{F1} - Y_{eth,F1}, \quad (17)$$

$$Y_{C,F2} = 1 - Y_{F2} - Y_{lac,F2}. \quad (18)$$

Appendix A explains how to obtain Eqs. (16)–(18).

For each metabolic pathway, the enthalpy changes for the aerobic and anaerobic microbial growth reactions are obtained by adding the enthalpies of the catabolic and anabolic reactions (Tables A.1 and A.2) multiplied by coefficients corresponding to the uptake of 1 C-mol of glucose (Aerobic: Eq. (A.4), F1: Eq. (A.5), and F2: Eq. (A.6)),

$$\Delta_i H_{glu} = (1 - Y_i Y_{ana}) \Delta_{cat,i} H_{glu} + Y_i \Delta_{ana} H_B, \quad (19)$$

where  $i$  can be AE, F1 or F2.  $Y_{ana}$  is the stoichiometric coefficient of the substrate in the anabolic reaction written for 1 C-mol of biomass; e.g., for glucose  $Y_{ana} = \frac{\gamma_B}{\gamma_{glu}}$  (Table A.2). The change in enthalpy of the anabolism,  $\Delta_{ana} H_B$ , is zero irrespective of the type of substrate, when constructing the growth reaction following the electron balance approach (Appendix A). The enthalpy change of catabolism under aerobic conditions can be written as a function of the DR of glucose ( $\gamma_{glu}$ ) using Thornton's rule (Appendix B):  $\Delta_{cat,AE} H_{glu} = \frac{\gamma_{glu}}{4} \Delta H_T$ , where  $\Delta H_T = -469$  kJ mol<sup>-1</sup> O<sub>2</sub> is Thornton's constant for glucose (Thornton, 1917). Since Thornton's rule is not valid in fermentative or anaerobic conditions, we used measured changes of enthalpies of catabolism in fermentation pathways F1 and F2 (Tables A.1 and A.2, respectively). Thus Eq. (19) is simplified to

$$\Delta_i H_{glu} = \left(1 - Y_i \frac{\gamma_B}{\gamma_{glu}}\right) \Delta_{cat,i} H_{glu}. \quad (20)$$

Similar to glucose, a microbial growth reaction for the uptake of SOM during aerobic metabolism can be written as,

$$C_{SOM} + \left(\frac{\gamma_{SOM} - Y_{SOM} \gamma_B}{4}\right) O_2 \xrightarrow{U_{SOM}} Y_{SOM} C_B + Y_{C,SOM} CO_2 + \Delta_{AE} H_{SOM}, \quad (21)$$

where  $U_{SOM}$ ,  $Y_{SOM}$ ,  $\gamma_{SOM}$  and  $\Delta_{AE} H_{SOM}$  are the rate of the reaction, the biomass yield (in C-mol biomass C-mol<sup>-1</sup> SOM), the DR of SOM, and the enthalpy change of the reaction (in kJ C-mol<sup>-1</sup> SOM), respectively.

$Y_{C,SOM}$  is the CO<sub>2</sub> yield, which is calculated as  $Y_{C,SOM} = 1 - Y_{SOM}$ .  $\Delta_{AE} H_{SOM}$  can be estimated using a similar equation as Eq. (20), as

$$\Delta_{AE} H_{SOM} = \left(1 - Y_{SOM} \frac{\gamma_B}{\gamma_{SOM}}\right) \Delta_{cat,AE} H_{SOM}, \quad (22)$$

where  $\Delta_{cat,AE} H_{SOM} = \frac{\gamma_{SOM}}{4} \Delta H_T$ , and  $\Delta H_T = -455 \pm 15$  kJ mol<sup>-1</sup> O<sub>2</sub> is Thornton's constant for organic compounds other than glucose (Thornton, 1917). The DR of SOM is generally not known a priori and has to be obtained experimentally (Boye et al., 2017).

Since Eqs. (20) and (22) use two different values of Thornton's constant, we use Eq. (B.1) to define two different values of the DR of microbial biomass to ensure the same enthalpy of combustion of biomass in all the analyses ( $\Delta_C H_B = -492$  kJ C-mol<sup>-1</sup> of biomass) as  $\gamma_B = \frac{\Delta_C H_B}{-469} = 4.2$  and  $\gamma_B = \frac{\Delta_C H_B}{-455} = 4.32$ , respectively. Therefore, to summarize, when analyzing the metabolism of glucose, we used  $\Delta H_T = -469$  kJ mol<sup>-1</sup> O<sub>2</sub> with  $\gamma_B = 4.2$ , whereas for substrate other than glucose, we used  $\Delta H_T = -455$  kJ mol<sup>-1</sup> O<sub>2</sub> with  $\gamma_B = 4.32$ .

Eqs. (10)–(21) describe the mass and energy balances during microbial growth on glucose and SOM. The known parameters in this system of equations are the DR of glucose, biomass, ethanol and lactic acid ( $\gamma_{glu}$ ,  $\gamma_B$ ,  $\gamma_{eth}$  and  $\gamma_{lac}$ ), and the changes of enthalpies of catabolism and anabolism of the three metabolic pathways ( $\Delta_{cat,i} H_{glu}$ ,  $\Delta_{ana} H_B = 0$ ). The unknown parameters are the growth yields of the purely aerobic reaction ( $Y_{AE}$ ) and the two fermentation reactions ( $Y_{F1}$  and  $Y_{F2}$ ), as well as the fractional rates  $\alpha$  and  $\beta$  (recall that  $\lambda = 1 - \alpha - \beta$ ). If SOM uptake is also taken into consideration, then additional unknown parameters are  $U_{SOM}$ ,  $Y_{SOM}$ ,  $\gamma_{SOM}$ , and  $r_p$ . In the following sections,  $U_{glu}$  and  $U_{SOM}$  do not appear as model parameters because we only use the fractional rates. Now we can let these unknown parameters vary and study the behavior of CR as different metabolic pathways dominate, or varying substrate type and CUE.

### 3. Calorespirometric ratio and carbon use efficiency during glucose metabolism

#### 3.1. Calorespirometric ratio and glucose metabolic pathways

To answer our second question, Eq. (8) is used to study how CR varies as a function of the rates of substrate uptake and metabolism along the different pathways when microbial growth is either negligible (Section 3.1.1) or an important contribution to the enthalpy changes (Section 3.1.2). We start by considering the case of large substrate additions and negligible priming, so that  $U_{SOM} \approx 0$  (i.e.,  $r_p \approx 0$ ). In this case, the CR from Eq. (8) can be further simplified to,

$$CR = -\frac{\alpha \Delta_{AE} H_{glu} + \beta \Delta_{F1} H_{glu} + \lambda \Delta_{F2} H_{glu}}{Y_{CO_2}}. \quad (23)$$

The effect of different metabolic pathways on CR is assessed in the following sections by varying  $\alpha$  and  $\beta$  (recall that  $\lambda = 1 - \alpha - \beta$ ).

**Table 3**  
Calorespirometric ratio in systems with negligible microbial growth.

Metabolic pathway	Range of fractional rates	Calorespirometric ratio	Catabolic reaction
Only aerobic	$\alpha = 1, \beta = 0, \lambda = 0$	$-\Delta_{cat,AE} H_{glu} = -\frac{\gamma_{glu}}{4} \Delta H_T$	$CH_2O_{(glu)} + O_2 \rightarrow CO_2$
Only fermentation F1	$\alpha = 0, \beta = 1, \lambda = 0$	$-\frac{\Delta_{cat,F1} H_{glu}}{1 - \frac{\gamma_{glu}}{\gamma_{eth}}}$	$CH_2O_{(glu)} \rightarrow \frac{\gamma_{glu}}{\gamma_{eth}} CH_3O_{0.5(eth)} + \left(1 - \frac{\gamma_{glu}}{\gamma_{eth}}\right) CO_2$
Only fermentation F2	$\alpha = 0, \beta = 0, \lambda = 1$	Infinity	$CH_2O_{(glu)} \rightarrow CH_2O_{(lac)}$
Combined fermentation	$\alpha = 0, \beta < 1, \lambda = 1 - \beta$	$-\frac{\Delta_{cat,F1} H_{glu} + \frac{\lambda}{\beta} \Delta_{cat,F2} H_{glu}}{1 - \frac{\gamma_{glu}}{\gamma_{eth}}}$	Catabolism of glucose to CO <sub>2</sub> , ethanol, and lactic acid
Combined aerobic and fermentation	All >0 and <1	$-\frac{\alpha \Delta_{cat,AE} H_{glu} + \beta \Delta_{cat,F1} H_{glu} + \lambda \Delta_{cat,F2} H_{glu}}{\alpha + \beta \left(1 - \frac{\gamma_{glu}}{\gamma_{eth}}\right)}$	Catabolism of glucose to CO <sub>2</sub> , ethanol, and lactic acid

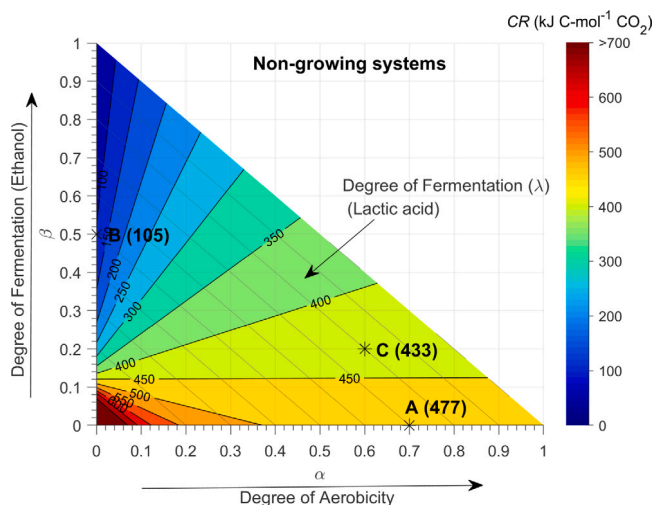


**Fig. 3.** Calorespirometric ratio (CR) for soils with negligible microbial growth, as a function of the fractional rates of aerobic and fermentation pathways F1 and F2. The degree of aerobicity  $\alpha$  increases on the x-axis from 0 (only fermentation) to 1 (only aerobic metabolism on glucose; CR = 469 kJ C-mol<sup>-1</sup> CO<sub>2</sub>). The degree of fermentation via F1 pathway  $\beta$  increases from 0 to 1 on the y-axis (only fermentation metabolism on glucose with ethanol as the end product; CR = 50.1 kJ C-mol<sup>-1</sup> CO<sub>2</sub>). Variation along the diagonal represents the fractional rate of metabolism following F2 pathway ( $\lambda = 1 - \alpha - \beta$ ), ranging from  $\lambda = 0$  (only aerobic and F1 metabolism) to 1 at the origin, where  $\alpha = \beta = 0$  (only F2 pathway is active and no CO<sub>2</sub> is produced; CR approaches infinity). Points A, B and C are explained in detail in the text, and the values in parentheses are the values of CR in kJ C-mol<sup>-1</sup> CO<sub>2</sub> at these points.

### 3.1.1. Calorespirometric ratio in soils with negligible microbial growth

In calorimetric experiments designed to study basal microbial activity, heat measurements are typically collected in the early lag phase of microbial growth (Herrmann and Bölscher, 2015) or in the late steady state phase with the assumption that substrate is only used for maintenance and not for growth (Barros et al., 2011). Thus, in these experiments the substrate is catabolized only to produce free energy to overcome the maintenance requirements and growth yields are negligible (Tijhuis et al., 1993). Setting growth yields  $Y_{AE}$ ,  $Y_{F1}$  and  $Y_{F2}$  to zero, calculating the enthalpy changes with Eq. (20), and substituting in Eq. (23), the CR can be written as,

$$CR = -\frac{\alpha \Delta_{AE} H_{glu} + \beta \Delta_{F1} H_{glu} + \lambda \Delta_{F2} H_{glu}}{\alpha + \beta(1 - Y_{eth,F1})} \quad (24)$$

Inserting the value of  $Y_{eth,F1}$  from Eq. (A.7) in Eq. (24), we obtain CR as a function of fractional rates,

$$CR = -\frac{\alpha \Delta_{AE} H_{glu} + \beta \Delta_{F1} H_{glu} + \lambda \Delta_{F2} H_{glu}}{\alpha + \left(1 - \frac{\gamma_{glu}}{\gamma_{eth}}\right) \beta} \quad (25)$$

The effect on CR of catabolism along different pathways is explored in Fig. 3, and the corresponding mathematical expressions are summarized in Table 3. In Fig. 3, the fractional rates of aerobic, ethanol fermentation and lactic acid fermentation increase from zero to one along the x-axis, y-axis and the diagonal direction (towards the origin), respectively. At a degree of aerobicity  $\alpha = 1$ , glucose metabolism is completely aerobic and CR is equal to the enthalpy change of catabolism of 1 C-mol of glucose to CO<sub>2</sub>; i.e., 469 kJ C-mol<sup>-1</sup> CO<sub>2</sub> (Wadsö and Hansen, 2015). Similarly, at a degree of fermentation  $\beta = 1$ , only ethanol fermentation occurs and CR is equal to the enthalpy change of catabolism of 1 C-mol of glucose to ethanol; i.e., 50.1 kJ C-mol<sup>-1</sup> CO<sub>2</sub>. With a degree of fermentation  $\lambda = 1$ , only lactic acid fermentation occurs and CR is infinity because no CO<sub>2</sub> is produced. These three extreme cases are represented by the vertices of the triangle shown in Fig. 3. Points along the edges are characterized by the co-occurrence of two pathways. As we move from  $\alpha = 1$  to  $\alpha = 0$  along the x-axis soils become more deprived of electron acceptors (either O<sub>2</sub> or inorganic), fermentation become dominant, and CR approaches infinity. Similarly, as we move from  $\beta = 1$  to  $\beta = 0$  along the y-axis soils becomes dominated by lactic-acid producing microorganism and CR approaches infinity. All other points (colored area) represent combinations of these three pathways.

For illustration, let us select three points in Fig. 3: A, B and C (represented by asterisks). At point A, glucose is metabolized 70% aerobically and 30% via fermentation pathway F2, and CR = 477 kJ C-mol<sup>-1</sup> CO<sub>2</sub>. This value is slightly higher than that attained under completely aerobic conditions because lactic acid fermentation F2 produces a small amount of heat, but no CO<sub>2</sub>. At point B, glucose is metabolized 50% via F1 and 50% via F2, and CR = 105 kJ C-mol<sup>-1</sup> CO<sub>2</sub>. This value is also higher than in the case of only F1 fermentation because F2 fermentation does not produce CO<sub>2</sub>. At point C, glucose metabolism proceeds through all three pathways, with 60% aerobic, 20% F1 and 20% F2 resulting in CR = 433 kJ C-mol<sup>-1</sup> CO<sub>2</sub>. This analysis highlights large variations of CR even under basal metabolism with negligible growth.

In the following section, we relax the assumption of basal metabolism, and analyze how the CR changes when microbial growth occurs, as a function of fractional rates as well as microbial growth yields associated with each metabolic pathway.

### 3.1.2. Calorespirometric ratio in soils with microbial growth

In contrast to basal metabolism, a growing microbial biomass partitions free energy obtained from catabolism to both biosynthesis and

**Table 4**  
Calorespirometric ratio in systems with microbial growth.

Metabolic pathway	Range of fractional rates	Calorespirometric ratio	Growth reaction
Only aerobic	$\alpha = 1, \beta = 0, \lambda = 0$	$-\frac{\Delta_{AE}H_{glu}}{1 - Y_{AE}}$	Eq. (A.4)
Only fermentation F1	$\alpha = 0, \beta = 1, \lambda = 0$	$-\frac{\Delta_{F1}H_{glu}}{1 - Y_{F1} - Y_{eth,F1}}$	Eq. (A.5)
Only fermentation F2	$\alpha = 0, \beta = 0, \lambda = 1$	$-\frac{\Delta_{F2}H_{glu}}{1 - Y_{F2} - Y_{lac,F2}}$	Eq. (A.6)
Combined fermentation	$\alpha = 0, \beta < 1, \lambda = 1 - \beta$	$-\frac{\beta \Delta_{F1}H_{glu} + \lambda \Delta_{F2}H_{glu}}{\beta(1 - Y_{F1} - Y_{eth,F1}) + \lambda(1 - Y_{F2} - Y_{lac,F2})}$	Catabolism of glucose to CO <sub>2</sub> , ethanol, as well as lactic acid
Combined aerobic and fermentation	All >0 and <1	Eq. (23)	Catabolism of glucose to CO <sub>2</sub> , ethanol, as well as lactic acid

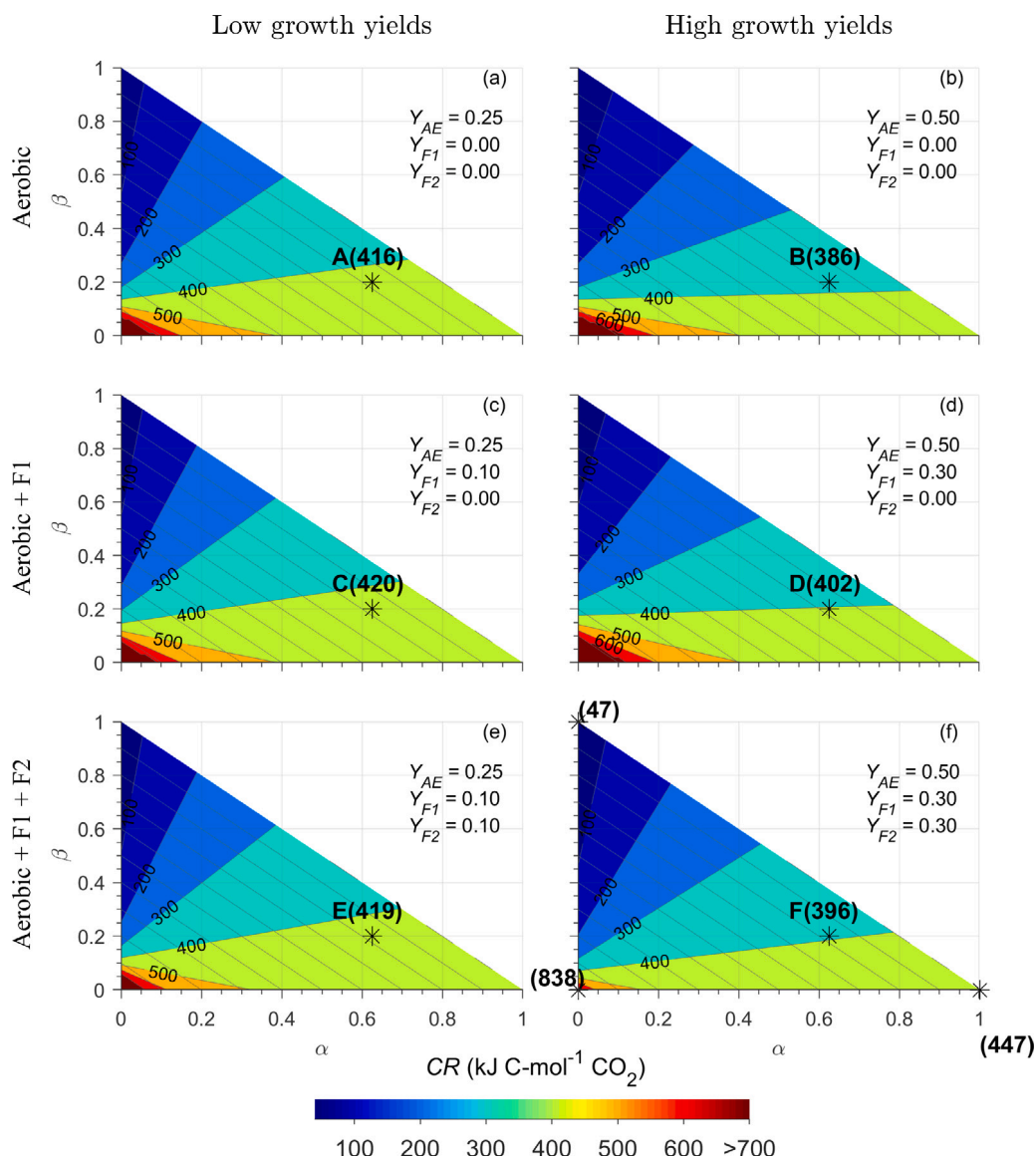


**Fig. 4.** Calorespirometric ratio (CR) for soils with microbial growth, as a function of fractional rates of aerobic ( $\alpha$ ) and fermentation pathways F1 ( $\beta$ ) and F2 ( $\lambda$ ). Panels on the left refer to microbial growth with low yield values, and panels on the right refer to high yield values. The three rows show the effect of microbial growth in mixed metabolisms on CR: aerobic growth (a, b), aerobic + F1 growth (c, d) and aerobic + F1 + F2 growth (e, f). Note that all three metabolic pathways are active in all panels, but biomass is growing using a given pathway only if the corresponding yield value is larger than zero (indicated on the right of each panel). Values in parentheses are the values of CR in kJ C-mol<sup>-1</sup> CO<sub>2</sub> for specific points described in the text.

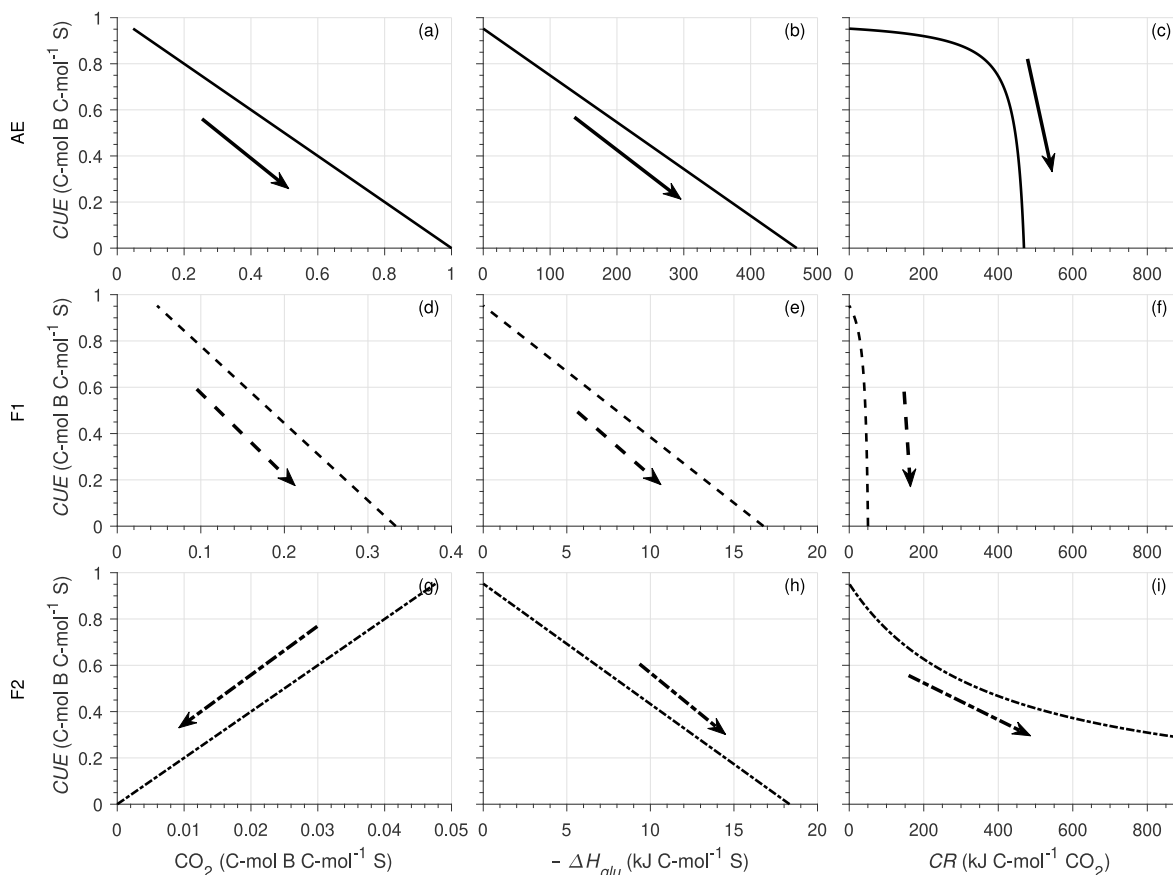


Fig. 5. Variations of CUE with  $\text{CO}_2$  yield (a,d and g), enthalpy change during microbial growth (expressed in absolute value; b,e, and h), and CR (c,f, and i) for AE, F1 and F2 pathways under scenario one in Section 3.1.2. In each panel, the growth yield corresponding to the different metabolic pathways is varied (decreasing) according to the arrow.

maintenance, assuming there is no overflow respiration or other losses of substrate. In this case, CR depends not only on the rates along the different metabolic pathways, but also on the individual growth yields for each of these pathways. Thus, parameters  $\alpha$ ,  $\beta$ ,  $\gamma$ , and yields  $Y_{AE}$ ,  $Y_{F1}$ , and  $Y_{F2}$  can vary independently and simultaneously. These yields do not appear explicitly in Eq. (23), but they affect the enthalpy changes via Eq. (20). As in Section 3.1.1, for completely aerobic metabolism, CR is obtained by evaluating Eq. (23) for values of  $\alpha = 1$ ,  $\beta = 0$  and  $\lambda = 0$ . Similarly, when only fermentation F1 or F2 occur, CR can be evaluated using values of  $(\alpha, \beta, \lambda)$  equal to  $(0, 1, 0)$  or  $(0, 0, 1)$ , respectively. In the case of combined fermentation pathways, F1 and F2 occur simultaneously and CR is given by Eq. (23) for  $\alpha = 0$  and  $\beta + \lambda = 1$ . In this case, either  $\beta$  or  $\lambda$  is enough to calculate CR. The resulting expressions are summarized in Table 4, and variations in CR for different combinations of these pathways are illustrated in Fig. 4.

Fig. 4 is similar to Fig. 3, except that here CR is shown as a function of both fractional rates and growth yields of the different metabolic pathways because now microbial growth cannot be neglected. The two columns, characterized by low growth yield (left) and high growth yield (right), show the variation of CR with  $\alpha$  and  $\beta$  for the three metabolic pathways: only aerobic (Fig. 4a and b), aerobic and F1 (Fig. 4c and d), and aerobic, F1 and F2 (Fig. 4e and f). For example, for only aerobic or only fermentative (F1 or F2) pathways, CR = 445.5, 47.2, and 837 kJ  $\text{C-mol}^{-1} \text{CO}_2$ , respectively (assuming yield values as given in Fig. 4f; i.e.,  $Y_{AE} = 0.5$ ,  $Y_{F1} = 0.3$ , and  $Y_{F2} = 0.3$ ).

CR values do not vary significantly when aerobic and fermentation pathways are combined. This becomes clear by comparing the CR values in the low growth yield column (see star symbols A, C, and E in Fig. 4a, c, and e) and in the high growth yield column (star symbols B, D, and F in Fig. 4b, d, and f). Combining fermentation with aerobic metabolism (Fig. 4a vs. c and e; and Fig. 4b vs. d and f) has minor

effects on CR because the catabolism of glucose in fermentation releases much less heat and  $\text{CO}_2$  compared to the aerobic pathway (Table A.1). However, as fermentation F2 metabolism becomes dominant, CR values increase rapidly because negligible amounts of  $\text{CO}_2$  are produced during lactic acid metabolism, resulting in a very high CR. In contrast, variations in growth yield have a larger impact on the CR (compare Fig. 4a vs. 4b; 4c vs. 4d; and 4e vs. 4f).

To further illustrate the effects of varying growth metabolic pathways (as done in Fig. 3), we select three points B, D, and F in Fig. 4b, d, and f, respectively. At point B, microorganisms are growing only via the aerobic pathway; however, catabolism of glucose via F1 and F2 also occurs, but it does not result in growth because we assumed that  $Y_{F1}$  and  $Y_{F2}$  are zero. Under these conditions, CR = 385 kJ  $\text{C-mol}^{-1} \text{CO}_2$ . At point D, microorganisms are growing aerobically as well as via the F1 pathway. Also, in this case, catabolism of glucose via the F2 pathway occurs, but we assumed that it does not result in growth. CR at point D is 401 kJ  $\text{C-mol}^{-1} \text{CO}_2$ . At point F, microorganisms grow using all three metabolic pathways and CR = 395 kJ  $\text{C-mol}^{-1} \text{CO}_2$ .

### 3.2. Calorespirometric ratio and carbon use efficiency

In this section, we address questions 3 and 4 presented in the introduction, namely, (i) on the relationship between the CR and CUE 3.2.1 and (ii) on the effect of priming on this relationship 3.2.2. To do this, we need a generalized expression linking CR to CUE, instead of the growth yields of the individual pathways. For CR, we have already derived an expression in Section 3.1 given by Eq. (23), and now we formulate a general expression for CUE from Eqs. (5), (11) and (21) as follows,

$$CUE = \frac{Y_{glu}U_{glu} + Y_{SOM}U_{SOM}}{U_{glu} + U_{SOM}}, \quad (26)$$

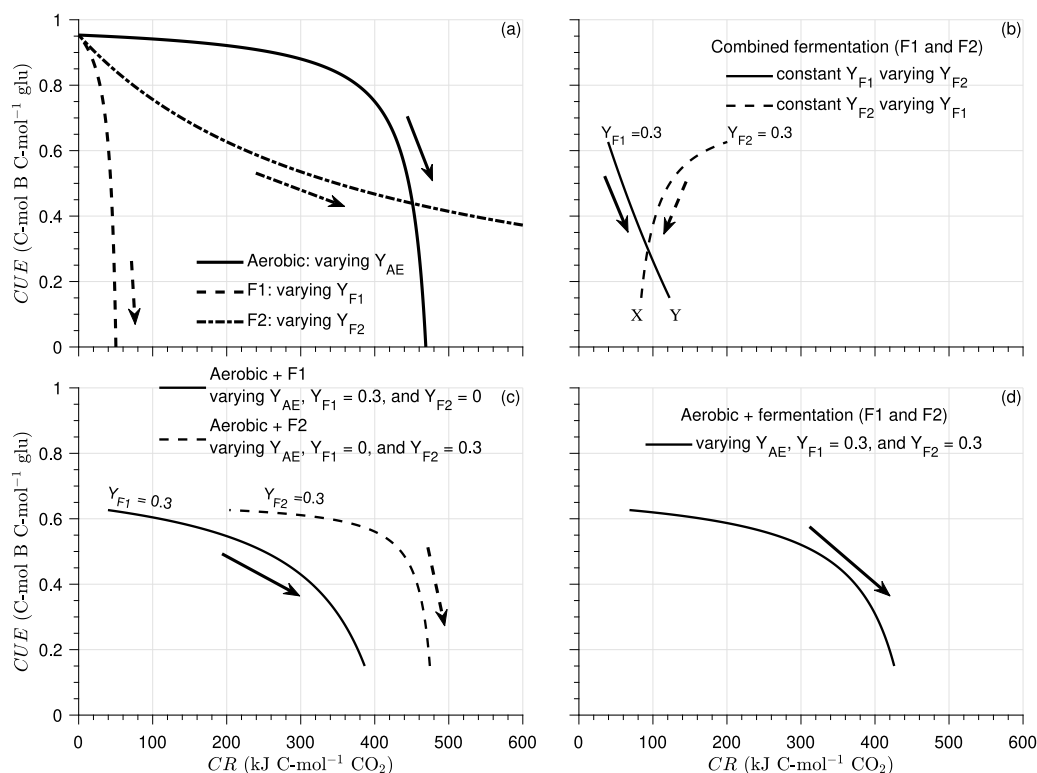


**Fig. 6.** Carbon use efficiency (CUE) as a function of calorespirometric ratio (CR) for different glucose metabolic pathways; curves are obtained by plotting CUE and CR as one growth yield is varied as indicated: (a) only one metabolic pathway is active: AE ( $\alpha = 1$ ,  $\beta = 0$ , and  $\lambda = 0$ ), F1 ( $\alpha = 0$ ,  $\beta = 1$ , and  $\lambda = 0$ ) or F2 ( $\alpha = 0$ ,  $\beta = 0$ , and  $\lambda = 1$ ), (b) only fermentation F1 and F2 pathways ( $\alpha = 0$ ,  $\beta = 0.5$ , and  $\lambda = 0.5$ ), (c) aerobic with F1 ( $\alpha = 0.5$ ,  $\beta = 0.5$ , and  $\lambda = 0$ ) and aerobic with F2 ( $\alpha = 0.5$ ,  $\beta = 0$ , and  $\lambda = 0.5$ ) pathways, and (d) all three pathways ( $\alpha = 0.5$ ,  $\beta = 0.25$ , and  $\lambda = 0.25$ ). In each panel, one of the growth yields (as indicated by the legend) is varied (decreasing) according to the arrow.

where we set  $U_{SOM} = 0$  because here we only consider the metabolism of glucose, and  $Y_{glu}$  is given by Eq. (11). Therefore, CUE is given by

$$CUE = Y_{glu} = \alpha Y_{AE} + \beta Y_{F1} + \lambda Y_{F2}. \quad (27)$$

Both Eqs. (26) and (27) essentially define CUE as weighted averages of the growth yields for all reactions leading to microbial growth. The  $Y_{glu}$  is constrained by the energy available for anabolism (i.e., the DR of the substrate). Accordingly, the maximum  $Y_{glu}$  (denoted as  $Y_{glu}^{max}$ ) is calculated based on the thermodynamic limit for the growth yields of each metabolic pathway ( $Y_{i,glu}^{max} = 0.95 \text{ C-mol B C-mol}^{-1} \text{ glu}$  with  $i = \text{AE, F1, F2}$ ; see Appendix C). The  $Y_{glu}^{max}$  set limits to the thermodynamically feasible range of variation in the CUE–CR relations presented in the following sections. It should be noted that for each pathway, the maximum yields are theoretical values that in reality are not achieved. For example, under aerobic conditions, growth yields are often found in the range of 0.4–0.8, and values lower than 0.4 generally suggest that microorganisms are under stress (Smeaton and Van Cappellen, 2018) or under nutrient limitation (Manzoni et al., 2017). Similarly, under anaerobic conditions, growth yields are in the range of 0–0.3 (Smeaton and Van Cappellen, 2018).

### 3.2.1. CUE Vs. CR under different glucose metabolic pathways

After analyzing CR as a function of the uptake rates in different pathways for given growth yields (Fig. 4), here we describe the relationship between CUE (Eq. (27)) and CR (Eq. (23)), when growth yields in different metabolic pathways are varied for given uptake rates. Because interpreting the relation between CUE and CR is complicated by the numerous concurrent processes controlling this connection, we start by illustrating how the two components of CR (heat and  $\text{CO}_2$  exchange rates) vary with CUE in individual metabolic pathways for microbial growth (Fig. 5). This analysis allows us explaining CUE–CR relations in four scenarios characterized by different combinations of metabolic pathways (Fig. 6): (1) only one pathway (i.e., either AE, F1

or F2; Fig. 6a), (2) both fermentation pathways (F1 and F2; Fig. 6b), (3) aerobic and one of the fermentation pathways (AE and F1 or F2; Fig. 6c), and (4) all pathways combined (AE, F1, and F2; Fig. 6d).

Fig. 5 shows the variation of CUE with the amount of  $\text{CO}_2$  (left panels) and heat released (middle panels), and with CR (right panels) during metabolism of glucose via the aerobic pathway (solid black line; top panels), the fermentation F1 (dashed line, middle panels), and the fermentation F2 (dotted–dashed line, bottom panels) pathways. Because a single metabolic pathway is considered in each set of panels, the CUE values are the same as the growth yields for each pathway; i.e.,  $Y_{AE}$ ,  $Y_{F1}$ , or  $Y_{F2}$ . The analytical expressions of CUE–CR relationships for all three pathways are reported in Table 4. In the AE and F1 pathways, the amount of  $\text{CO}_2$  (panels a, d, and g) produced increases with decreasing CUE, whereas in the F2 pathway it decreases because  $\text{CO}_2$  is produced from the anabolic reaction. The amount of heat released (panels b, e, and h) and CR (panels c, f, and i) increases with decreasing CUE in all three pathways. At the maximum value of CUE, CR is equal to zero because the enthalpy content of glucose is completely transferred to biomass. When that happens,  $\Delta_{AE} H_{glu} = \Delta_{F1} H_{glu} = \Delta_{F2} H_{glu} = 0$  and no heat is released, causing CR to become zero. In this case, the maximum value of CUE is 0.95, as calculated in Appendix C. It should be noted that the value of zero CR at the maximum values of CUE is theoretically valid, but it would be physiologically impossible for microorganisms because they need to respire  $\text{CO}_2$  in order to grow.

In all three pathways, as CUE decreases, CR increases because the heat dissipation increases faster than  $\text{CO}_2$  production rate. When growth stops (i.e.,  $CUE = 0$ ), the CR is maximized, and glucose is metabolized only for maintenance purposes. In the F1 pathway, the range of variation of CR (Fig. 5f) is relatively small for a large variation of CUE compared to the AE pathway (Fig. 5e). This difference is due to the lower heat dissipation of the F1 pathway (Fig. 5b and e) and similar production of  $\text{CO}_2$  (Fig. 5a and d) compared to the AE pathway.

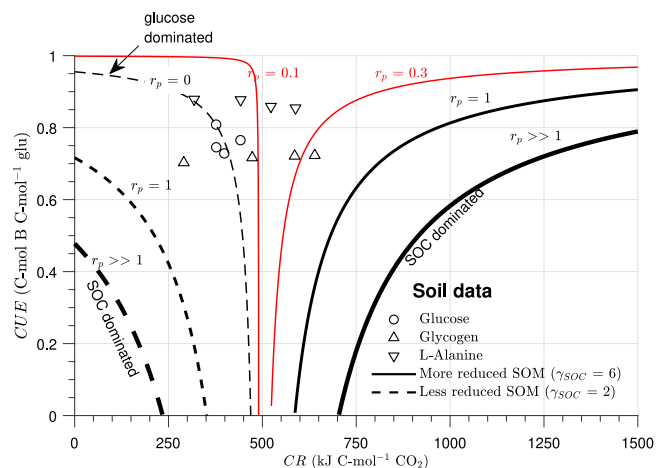


**Fig. 7.** Carbon use efficiency (CUE) as a function of calorespirometric ratio (CR) when uptake of both the added substrate (glucose) and SOM are considered. Solid lines represent a more reduced SOM and dashed lines a less reduced SOM as compared to biomass. The thickness of the lines represents an increasing degree of priming as measured by the ratio of the rates of uptake of SOM and glucose under aerobic conditions ( $r_p$ ). The thin dashed line shows CUE variations in systems with no priming ( $r_p = 0$ ), equivalent to the aerobic metabolism of glucose (same as in the solid black line in Fig. 6a and 9). The thick dashed and solid lines with the annotation ‘SOM dominated’ show CUE variations when SOM is the only C source. Priming occurs for intermediate values of  $r_p$ ; e.g.,  $r_p = 0.1, 0.3$  or  $1$ . Open symbols represent observed values of CR and growth yields estimated in four soils amended with different compounds (Table A.4) (Bölscher et al., 2016). The red lines illustrate that priming can explain the observed CUE and CR from Bölscher et al. (2016).

In the case of the F2 pathway, CR varies from zero at maximum CUE to infinity at minimum CUE even though the variation of heat dissipated is similar to the F1 pathway (Fig. 5h). In the F2 pathway, at the maximum value of CUE, the  $\text{CO}_2$  yield is a finite value ( $0.05 \text{ C mol CO}_2^{-1} \text{ C mol glu}$ ) and heat dissipation is zero, so CR is also zero. As CUE decreases, the  $\text{CO}_2$  yield decreases because more and more glucose is catabolized to lactic acid instead of  $\text{CO}_2$ . As a result, more heat is released per unit  $\text{CO}_2$  produced, until CR approaches infinity when CUE approaches zero.

Fig. 6a compares the CUE–CR relation for the first scenario, by combining information from panels e, f and i in Fig. 5. Fig. 6b shows the CUE–CR relation for the second scenario; i.e., the combined fermentation F1 and F2. The CUE and CR in this scenario change because the growth yields of F1 and F2 pathways vary, for given fractional rate  $\beta$  ( $\alpha = 0$  and  $\lambda = 1 - \beta$ ). By setting  $\beta = 0.5$  and using either  $Y_{F1}$  or  $Y_{F2}$  as a free parameter, we divide this scenario further into two cases. In the first case, CUE is calculated by fixing  $Y_{F1} = 0.3$  and varying  $Y_{F2}$  from zero to its maximum value 0.95 (indicated by the solid line in Fig. 6b). Thus, glucose is metabolized at a fixed F1 yield and a variable F2 yield, resulting in CUE decreasing with increasing CR. This behavior is similar to the dotted–dashed line in Fig. 6a, and the only difference here is that there is a constant supply of heat and  $\text{CO}_2$  from the F1 pathway at fixed  $Y_{F1} = 0.3$ . As  $Y_{F2}$  decreases (in the direction of the arrow), the CUE decreases, and the total heat (Eq. (15)) is produced at a faster rate compared to total  $\text{CO}_2$  (Eq. (14)), that results in increasing CR, despite the supply of heat and  $\text{CO}_2$  from F1. Moreover, at the minimum value of CUE ( $= \beta \times Y_{F1} + \gamma \times 0 = 0.15$ ), CR is a finite value as opposed to infinity in Fig. 6a. In the second case, CUE is calculated by fixing  $Y_{F2} = 0.3$  and varying  $Y_{F1}$  (indicated by the dashed line). In contrast to the first case, in the second case, the fermentation F2 pathway provides a constant source of heat and  $\text{CO}_2$  because  $Y_{F2}$  is fixed, which causes CUE to increase with increasing CR. The variation of CUE with the amount of  $\text{CO}_2$  and heat released, CR, and  $\beta$  are shown in Appendix D for both cases.

Fig. 6c shows the CUE–CR relation for the third scenario; i.e., the aerobic pathway combined with either fermentation F1 or F2. The CUE

and CR in this scenario depend on the growth yields of AE and either F1 or F2 pathways. By fixing  $\alpha = 0.5$  and using  $Y_{AE}$  as a free parameter, we divide this scenario further into two cases. In the first case (solid line), we consider the metabolism of glucose from both the AE and F1 pathways for  $\beta = 0.5$ ,  $\lambda = 0$ , and  $Y_{F1} = 0.3$  (letting  $Y_{AE}$  vary), while in the second case (dashed line), we consider the AE and F2 pathways for  $\beta = 0$ ,  $\lambda = 0.5$ , and  $Y_{F2} = 0.3$  (letting  $Y_{AE}$  vary). In both the cases, CUE decreases as CR increases, as when glucose is metabolized aerobically from the AE pathway dominates over the signal from the F1 or F2 pathway. However, the ranges of variability of CUE and CR are different in the third scenario compared to the first because of different values of the fractional rates.

Fig. 6d shows the CUE–CR relation for the fourth scenario; i.e., the aerobic pathway combined with both fermentation F1 and F2. The CUE and CR in this scenario are functions of growth yields and fractional rates in all pathways. For illustration, we fix the fractional rates  $\alpha = 0.5$ ,  $\beta = 0.25$ , and  $\lambda = 0.25$ , and the growth yields  $Y_{F2} = Y_{F1} = 0.3$ , using  $Y_{AE}$  as a free parameter to calculate CUE and CR. Similar to Fig. 6c, in this scenario CUE decreases as CR increase. This inverse relationship can be explained using the same argument as in Fig. 6c.

### 3.2.2. CUE Vs. CR under the effect of priming

In this section, we study the effect of priming on the relationship between CUE and CR under aerobic conditions, thus answering our fourth question. From Eqs. (8), (16), (21), and (26) with  $\alpha = 1$ ,  $\beta = 0$ , and  $\lambda = 0$ , we obtain

$$CR = -\frac{\Delta_{AE}H_{glu} + r_p\Delta_{AE}H_{SOM}}{1 - Y_{AE} + r_p(1 - Y_{SOM})}, \quad (28)$$

$$CUE = \frac{Y_{AE} + r_pY_{SOM}}{1 + r_p}, \quad (29)$$

where  $r_p$  had been defined earlier as the ratio between the uptake rates of SOM and glucose. Small (respectively large) values of  $r_p$  represent a low (respectively high) rate of uptake of SOM, and thus small (respectively large) priming. When the sources of variation in CUE and CR are the yields  $Y_{AE}$  and  $Y_{SOM}$ , we can solve Eqs. (28) and (29) by eliminating  $Y_{AE} + Y_{SOM}r_p$ , thus obtaining CUE as a function of CR as,

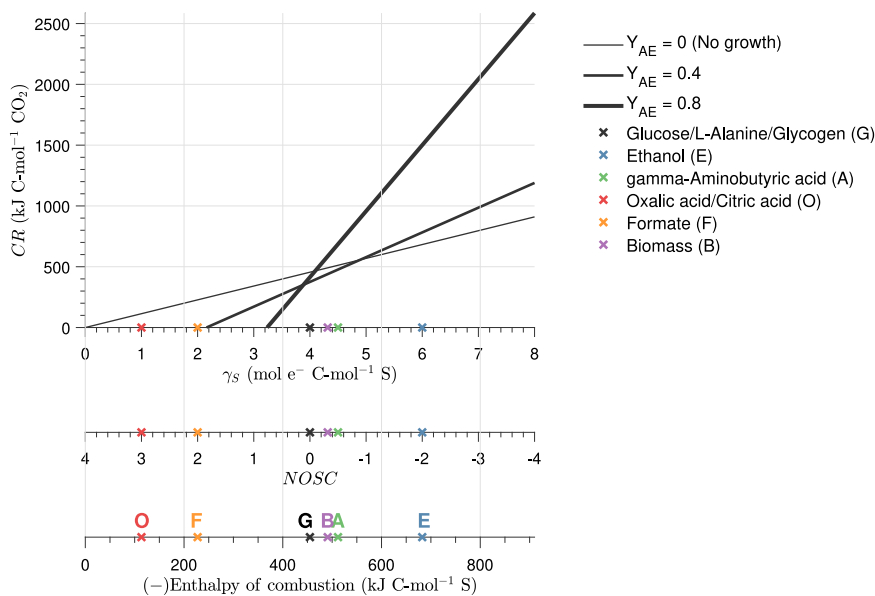
$$CUE = 1 + \frac{1}{CR} \left( \frac{\Delta_{AE}H_{glu} + r_p\Delta_{AE}H_{SOM}}{1 + r_p} \right). \quad (30)$$

Eq. (30) is still implicit in CUE because  $\Delta_{AE}H_{glu}$  and  $\Delta_{AE}H_{SOM}$  on the right hand side of the equation are functions of  $Y_{AE}$  and  $Y_{SOM}$ , respectively (Eq. (20) and (22)). An explicit form of CUE as a function of CR and the degrees of reduction of glucose and SOM can be found by substituting  $\Delta_{AE}H_{glu}$  from Eq. (20) and  $\Delta_{AE}H_{SOM}$  from Eq. (22), and using again Eq. (29),

$$CUE = \frac{CR + \left( \frac{\gamma_{glu} + r_p\gamma_{SOM}}{1 + r_p} \right) \frac{\Delta H_T}{4}}{CR + \frac{\gamma_B \Delta H_T}{4}}. \quad (31)$$

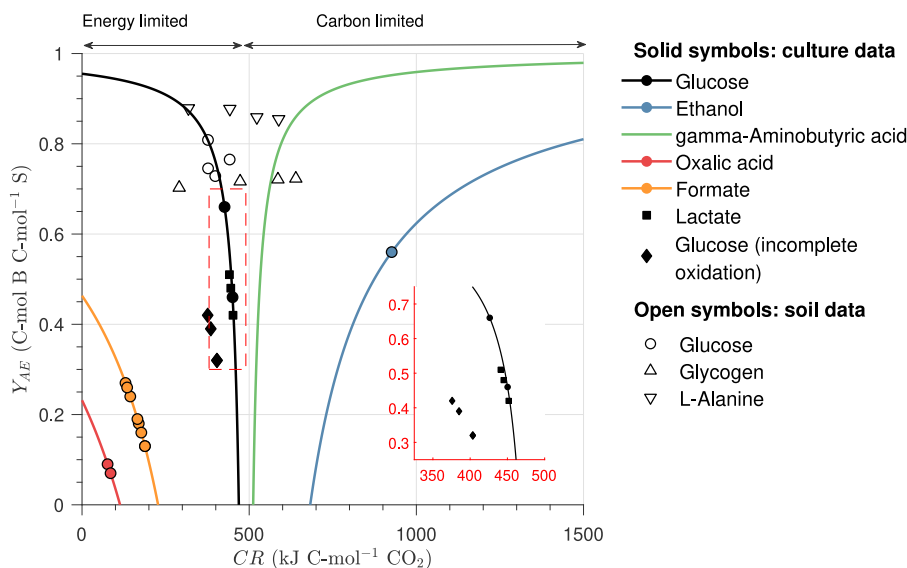
Note that if  $r_p = 0$ , then Eq. (31) reduces to Eq. (34), as discussed in Section 4.2.

Fig. 7 shows the CUE–CR relationships at varying degrees of priming for two different types of SOM—one is less reduced than biomass ( $\gamma_{SOM} = 2$ , dashed line) and the other is more reduced ( $\gamma_{SOM} = 6$ , solid line). For SOM with lower DR than biomass, CUE decreases with increasing CR like for glucose (compare to the solid curve in Fig. 6a), whereas SOM with higher DR than biomass causes CUE to increase with CR, like for ethanol (as discussed in Section 4). The anabolism of 1 C-mol of biomass requires 1 C-mol of SOM based on carbon stoichiometry; however, in the first case, 1 C-mol of SOM with  $\gamma_{SOM} < \gamma_B$  does not have enough electrons that are required in the anabolic reaction. In other words, growth is energy limited (see Appendix C). Thus, to increase their growth yield, microorganisms need to catabolize more



**Fig. 8.** Calorespirometric ratio (CR) as function of substrate degree of reduction (DR =  $\gamma_S$ ) in aerobic conditions at different levels of  $Y_{AE}$ , as indicated by solid lines of increasing thickness with increasing growth yields. Cross symbols of different colors are the DR of selected organic compounds; e.g.,  $\gamma_{glu} = 4$  (black),  $\gamma_{eth} = 6$  (blue), and  $\gamma_B = 4.2$  (purple). The additional x-axes show the corresponding values of the nominal oxidation state of C (NOSC =  $4 - \frac{DR}{C}$ , where C is the number of carbon atoms in the substrate) and the enthalpy of combustion corresponding to each  $\gamma_S$ . The enthalpy of combustion is calculated using Thornton's rule,  $\Delta_C H_{glu} = \frac{\gamma_S}{4} \Delta H_T$  where  $\Delta H_T = 469 \text{ kJ mol}^{-1} \text{ O}_2$  is the Thornton's constant.

The growth yield for a given substrate DR,  $Y_{AE}$ , is constrained by  $0 \leq Y_{AE} \leq \min\left(\frac{\gamma_S}{\gamma_B}, 1\right)$ , this is why not all black lines start from the origin (see Appendix C).



**Fig. 9.** Growth yield ( $Y_{AE}$ ) as a function of calorespirometric ratio (CR) for different substrates (see legend) in aerobic conditions. For substrates that are less reduced than biomass (e.g., glucose),  $Y_{AE}$  decreases with increasing CR, whereas for substrates that are more reduced than biomass (e.g., ethanol),  $Y_{AE}$  increases with increasing CR. Solid symbols represent the aerobic growth yields estimated from culture studies for which the corresponding CR is calculated using Eq. (32) (Table A.3). Solid diamonds represent aerobic growth on lactic acid (DR = 4) and solid squares refer to aerobic growth on glucose, but with acetate as an additional product of catabolism. The dashed red box is enlarged in the bottom right. Open symbols are the same as in Fig. 7.

SOM to meet the energy demand for anabolism, so that less energy and less C are available to be released as heat and  $\text{CO}_2$ . However, the heat is released more slowly compared to  $\text{CO}_2$ , which results in a decrease in CR with increasing CUE. In the second case, 1 C-mol of SOM with  $\gamma_{SOM} > \gamma_B$  can provide more electrons that are required in the anabolic reaction, implying that energetic requirements for anabolism are always met, and the growth yield is limited by the C content of SOM (see Appendix C). Similar to the first case, to increase their growth yield, microorganisms need to catabolize more SOM; however, anabolic energy requirements are already met, so that more energy is dissipated

as heat, but the same amount of C is released as in the first case, thereby increasing the CR.

These general patterns, driven by changes in the DR of SOM, are compounded with changes in the relative proportion of SOM metabolism compared to glucose metabolism. The thickness of the lines in Fig. 7 represents this proportion, with the thickest dashed or solid lines indicating growth only on SOM (i.e.,  $r_p \gg 1$ ) and the thin dashed line indicating growth only on glucose without any priming (i.e.,  $r_p = 0$ ). In the case of no priming, microorganisms grow on glucose, and the growth yield is limited by the enthalpy content of glucose (Fig. C.1). At intermediate values of  $r_p \approx 1$ , glucose and SOM are taken up at

comparable rates, and the CUE–CR relation shifts from being direct to inverse, depending upon the DR of SOM (solid and dashed lines of intermediate thickness). When SOM uptake is the dominant process ( $r_p \gg 1$ ), the effect of the DR of SOM is maximized, leading to the lowest CUE values for a given CR (thickest solid and dashed lines).

The potential effect of priming on the interpretation of CR data is explored in Fig. 7 by comparing CR and CUE from Bölscher et al. (2016) (Table A.4) to theoretical predictions using Eq. (31). CR and CUE data are presented as open triangles and circles, where the four points for each symbol category (circles and triangles) represent four different soil types. The data from soils amended with glucose (open circles) are close to the theoretically predicted black line. The data from experiments where L-Alanine and glycogen were added as substrates (upwards and downwards triangles) are also clustered around the black line because these compounds have DR = 4, like glucose. However, there are large deviations that might stem either from the different metabolism of L-Alanine and glycogen (which could cause larger heat production or lower CO<sub>2</sub> production than glucose, thereby increasing CR), or from priming. In fact, the data points overlap with the CUE–CR curves under different levels of priming (two red lines for  $r_p = 0.1$  and  $0.3$  in Fig. 7), showing that priming could explain the observed CR and CUE values. While we do not have data on the rate of uptake of SOM to confirm this result, we can conclude that priming is a potential candidate to explain deviations in the relationship between CUE and CR. This effect complicates the estimation of CUE from CR data because, in general,  $r_p$  is not known.

#### 4. Calorespirometric ratio for metabolism of other substrates under aerobic condition

##### 4.1. Calorespirometric ratio as a function of substrate degree of reduction

In this section, we describe the relationship between CR and CUE for different substrates and ignore the effect of priming. We consider a simple case with microbial growth under aerobic conditions, thus  $CUE = Y_{AE}$ , and CR can be obtained from Eqs. (8) and (16) for  $\alpha = 1$ ,  $\beta = 0$ ,  $\lambda = 0$  and  $r_p = 0$ . This results in an expression describing CR as a function of aerobic growth yield  $Y_{AE}$ ,

$$CR = -\frac{\Delta_{AE}H_S}{1 - Y_{AE}}, \quad (32)$$

where  $\Delta_{AE}H_S = \left(1 - Y_{AE}\frac{\gamma_B}{\gamma_S}\right)\Delta_{cat,AE}H_S$  is given by Eq. (20). In turn, the enthalpy change of catabolism can be written as a function of the DR of substrate using Thornton's rule,  $\Delta_{cat,AE}H_S = \frac{\gamma_S}{4}\Delta H_T$  (Appendix B). CR is thus obtained as a function of the DR of the substrate and the growth yield (Fig. 8),

$$CR = -\frac{\left(1 - Y_{AE}\frac{\gamma_B}{\gamma_S}\right)\frac{\gamma_S}{4}\Delta H_T}{1 - Y_{AE}}. \quad (33)$$

Increasing the DR of the substrate increases its enthalpy content, which means more energy is available to dissipate, causing a linear increase in CR (moving left to right in Fig. 8). This increase in CR with DR is observed irrespective of growing or non-growing conditions. In other words, either full or partial oxidation of 1 C-mol of methane (DR = 8) would produce more heat compared to oxalic acid (DR = 1), so that CR for methane is higher assuming the amount of CO<sub>2</sub> produced is not drastically different (Leak and Dalton, 1986; Rutgers et al., 1989). Different black lines show how CR varies as a function of growth yield—the thicker line the more efficient is microbial growth. In a growing system with  $Y_{AE} > 0$ , microbial growth only occurs when substrates contain enough energy; i.e.,  $\gamma_S \geq Y_{AE}\gamma_B$  (Heijnen and Roels, 1981). This constraint keeps  $CR > 0$  and causes the black lines to start from  $DR = \gamma_S = Y_{AE}\gamma_B$  in Fig. 8. For example, in the case of  $Y_{AE} = 0.4$  C-mol B C-mol<sup>-1</sup> S, microbial growth can only occur when the DR of the substrate is greater than  $0.4 \times \gamma_B = 1.68$ .

##### 4.2. CUE as a function of CR For different substrate degrees of reduction

Eq. (33) can also be used to estimate  $Y_{AE}$  from measured CR and  $\gamma_S$  (Fig. 9),

$$Y_{AE} = \frac{CR + \frac{\gamma_S}{4}\Delta H_T}{CR + \frac{\gamma_B}{4}\Delta H_T}. \quad (34)$$

This expression is analytically equivalent to the result by Hansen et al. (2004) and Wadsö and Hansen (2015), and can be applied to any substrate taken up in aerobic conditions to estimate  $Y_{AE}$  from the experimentally measured CR and substrate DR.

Increasing the growth yield decreases CR when the substrate is more oxidized than biomass and  $\gamma_S < \gamma_B$  (e.g., glucose, black line in Fig. 9). In contrast, when the substrate is more reduced than biomass and  $\gamma_S > \gamma_B$  (e.g., ethanol, blue line), increasing the growth yield increases CR. To explain this pattern, let us consider the examples of glucose and ethanol. For glucose as a substrate, the CUE–CR relation is the same as the solid line in Fig. 6a, and the explanation provided in Section 3.2.1 is valid here as well. For ethanol as substrate,  $Y_{AE}$  is maximum (i.e.,  $Y_{AE} = 0.95$ ; Appendix C) when CR approaches infinity because all the C content of the substrate is completely transferred to biomass and no CO<sub>2</sub> is produced. As  $Y_{AE}$  decreases, CO<sub>2</sub> production occurs at a faster rate compared to the rate at which heat is dissipated, which results in decreasing CR. The CR is minimized when growth stops, and ethanol is catabolized only for maintenance purposes. Variation of yield with CR for other substrates in Fig. 9 can be explained similarly.

To illustrate how  $Y_{AE}$  and CR could be related in hypothetical experiments, we used Eq. (32) to calculate the CR from the growth yields compiled by Smeaton and Van Cappellen (2018) for several organic compounds under aerobic conditions (Table A.3). The obtained pairs of  $Y_{AE}$  and CR are shown in Fig. 9 as solid circles. Solid squares denote the growth on glucose with acetate production, and solid diamonds denote the growth on lactic acid (DR = 4) with acetate production. It is noteworthy to see that product formation reduces the biomass yield, and this deviation can, in principle, be captured by CR measurements (enlarged inset). For example, the diamond symbols in the enlarged inset represent the CUE–CR values when glucose is catabolized to CO<sub>2</sub> and acetate, resulting in decreased CUE and CR because a fraction of glucose and enthalpy of glucose is transferred to acetate formation.

## 5. Discussion

Simultaneous measurements of heat and CO<sub>2</sub> from soils have been used to estimate CR (Barros et al., 2010; Herrmann and Bölscher, 2015; Geyer et al., 2019), but the current theoretical approaches to explain the observed variability of CR in soils are limited to simple cases (Hansen et al., 2004; Wadsö and Hansen, 2015). Here we present an extension, validation, and application of previous theories on the thermodynamics of microbial growth (Roels, 1983; Hansen et al., 2004; Von Stockar et al., 2006) to explain CR patterns in soils. Building on these previous contributions, we couple C and energy flows in a general framework that links CR to uptake and metabolism of added substrates and native organic matter, and microbial growth in soils. We use this framework to analyze the effects of different metabolic pathways (their rates and pathway-specific growth efficiencies; Figs. 3, 4, and 6), priming of SOM (Fig. 7), and substrate quality (Figs. 8 and 9), on CR and CUE. We emphasize that theories on microbial growths using thermodynamics are well established (Battley, 1960a; Westerhoff et al., 1982; Von Stockar et al., 2006), but the adoption of these thermodynamic theories is complex systems such as soils is in its infancy. Moreover, the modeling framework presented here allows for recovering numerous previous results by imposing specific assumptions. Therefore, some of our findings are not entirely new, but they are now placed into a general synthesis that is relevant to soils. However, linking CR to fermentation pathways and priming effect in soils has not been attempted before and thus represents a novel development.

### 5.1. General model behavior and its limitations

In systems where microbial growth can be neglected, CR depends only on the rates of the different metabolic pathways (Fig. 3); in contrast, in systems exhibiting microbial growth, CR is a function of rates as well as growth yields for each metabolic pathway (Fig. 4). In fact, substrate quality controls the energy availability for microbes via its enthalpy content (expressed by the DR) (Erickson, 1987; Amenabar et al., 2017; Boye et al., 2017), which in turn affects CUE and respiration rates (Gommers et al., 1988; Manzoni et al., 2012). The effect of substrate DR on heat dissipation is well-known (Roels, 1980a; Von Stockar et al., 2006), and hence it is not surprising that DR ultimately determines the CR (Fig. 8). All these parameters (CR, CUE, rates) are thus related, as shown in earlier studies (Hansen et al., 2004). The use of the coupled mass and energy balance model allowed us to express these relations mathematically, formulate CUE as a rate-weighted sum of growth yields for different metabolic pathways (Eqs. (5), (11), and (29)), and analytically link it to CR. Under aerobic conditions, the CUE–CR relationship (Eq. (34)) simplifies to a function that depends only on the substrate DR, which is analytically similar to that given by Hansen et al. (2004) and Wadsö and Hansen (2015). Here we have extended these previously proposed CUE–CR relationships by including metabolic pathways other than aerobic growth; i.e., the fermentation F1 and F2 pathways in systems with either negligible or significant microbial growth (Fig. 6) as well as the effects of priming (Fig. 7).

Besides the theoretical insights, this framework was tested by comparing the CR estimated by our model with the observed CR calculated from measured heat, biomass, CO<sub>2</sub>, and ethanol yields in a culture study under varying oxygen concentrations, where both aerobic and fermentation respiration occurred (von Stockar and Birou, 1989). The predicted CR values are close to the observations (Table C.1 and Fig. C.1), suggesting that our modeling framework is sufficiently detailed to capture variations in CR even in systems with combined metabolism. To keep the theory tractable, we have not considered the functional form of the uptake kinetics and its dependence on soil moisture and temperature conditions (Moyano et al., 2013; Keilueit et al., 2017). For example, the effect of non-standard temperature could be accounted for while estimating the enthalpy change of microbial growth reactions. These unaccounted environmental factors may affect heat production and respiration rates in different proportions, thus influencing CR (Barros et al., 2016a). These factors will also affect the relationship between CR and CUE when they alter the relative importance of certain processes—e.g., in saturated soils metabolism will shift from aerobic to anaerobic, leading to different CUE–CR relations.

### 5.2. Variation in calorespirometric ratio due to combined metabolic pathways and priming

Previous work suggests that CR should vary in the range 200–430 kJ C-mol<sup>-1</sup> CO<sub>2</sub> for microbial growth on glucose under purely aerobic conditions when the growth yield varies between 0.5–0.85 (Hansen et al., 2004). Note that higher values of CUE correspond to the lower value of CR because of the inverse CUE–CR relation for glucose in aerobic conditions (Fig. 6a). We found similar values: CR varies between 200–430 kJ C-mol<sup>-1</sup> CO<sub>2</sub> for  $Y_{AE}$  0.52–0.92 (Fig. 6a solid line), which can be attributed to a small disparity in the DR of microbial biomass, assumed to be 4.25 in (Hansen et al., 2004) and 4.2 here. Moreover, a practical range of variation of CR under completely aerobic conditions would be in the range 364–440 kJ C-mol<sup>-1</sup> CO<sub>2</sub> corresponding to aerobic CUE of 0.4–0.8. Values of CR outside this range are caused either by the occurrence of anaerobic metabolism or as a consequence of the catabolism of a substrate more reduced than glucose (Herrmann and Bölscher, 2015; Barros et al., 2011; Hansen et al., 2004). Both explanations are plausible based on our framework, but before discussing how our framework supports both of them, let us ask whether the CR range 364–440 kJ C-mol<sup>-1</sup> CO<sub>2</sub> implies perfect aerobic conditions for glucose

metabolism. If conditions are aerobic, then the CR would vary within this range; however, the opposite is not true because CR can vary within a similar range if fermentation of glucose also occurs (Fig. 6c and d). Therefore, the measurement of CUE together with CR could be useful to identify hidden metabolic pathways (see Section 5.3).

As hinted at above, our framework can help explain the variation of CR outside the range of perfect aerobic conditions. First, anaerobic metabolism (fermentation F1 or F2) increases CR values if fermentation F2 pathway is active (Figs. 3 and 4) because glucose is catabolized to lactic acid without any CO<sub>2</sub> production. However, the presence of fermentation F1 (i.e., glucose is catabolized to ethanol and CO<sub>2</sub>) decreases the CR compared to values attained under purely aerobic metabolism. The contributions from the glucose fermentation pathways are minor and could be neglected when considering well aerated soils. This is evident from Fig. 3 and 4, where the CR values are stable at high degrees of aerobicity. In contrast, for soils that are not well aerated, fermentation processes would have a larger impact on CR, as indicated by the blue shaded areas of Fig. 3 and 4. While here we have only considered fermentation F1 and F2 as anaerobic processes, depending upon the available electron acceptor or the microbial community structure, other anaerobic processes could also be active thereby affecting CR. For example, Boye et al. (2018) reported values of CR in soil samples amended with glucose from paddy fields, and the high CR values were attributed to the presence of anaerobic metabolism that resulted in heat production without proportional CO<sub>2</sub> release, as confirmed from the observed utilization of Fe<sup>3+</sup> and SO<sub>4</sub><sup>2-</sup> as electron acceptors. Since our framework does not include inorganic compounds as terminal electron acceptors, it cannot be used to interpret the data from Boye et al. (2018). Nonetheless, it can be used to derive expressions similar to Eq. (23) or (25) for anaerobic metabolism with other inorganic electron acceptors such as NO<sub>3</sub><sup>-</sup>, Fe(OH)<sub>3</sub>, SO<sub>4</sub><sup>2-</sup>, etc.

Second, CR values change when C sources other than the added substrate are metabolized aerobically either as a result of priming of SOM or another substrate (such as diauxic growth, la Cecilia et al. (2019)), as shown in Fig. 7. A higher value of CR is expected compared to growth only on glucose if the alternative C source is more reduced than glucose, and vice versa a lower CR value is expected for less reduced additional C sources. Being CR a ratio between rates, it is a highly sensitive metric. Therefore, to accurately interpret observed CR from soils, all the sources of C and energy that affect its value should be accounted for. The relations developed here provide a theoretical framework to assess the sensitivity of CR to all these contributions.

### 5.3. Predicting C-use efficiency from calorespirometric ratio

Building on previous work, we have shown that estimating CUE from CR is possible, provided that the dominant processes contributing to heat and CO<sub>2</sub> production are accounted for. However, this is not always possible, making an unambiguous estimation of CUE from CR alone difficult. The problems lie in the fact that different combinations of metabolic pathways can result in the same values of CR and CUE. This can be problematic when trying to estimate CUE or other parameters from measured CR because the same CR value can be caused by different processes. Our analysis shows that when the observed CR is supplemented by measurements of end-product yields, it is possible to identify the underlying metabolic pathways. For example, with reference to Fig. 6b, a CUE value of 0.15 and the corresponding CR = 84.19 and 122.5 kJ C-mol<sup>-1</sup> CO<sub>2</sub> can be achieved from two metabolic pathways, as indicated by points X and Y. The first combination is characterized by microorganisms growing via the fermentation F2 pathway with efficiency  $Y_{F2} = 0.3$  and using the fermentation F1 pathway only for catabolism (X in Fig. 6b). The second combination is characterized by microorganisms growing via fermentation F1 pathway with efficiency  $Y_{F1} = 0.3$  and using fermentation F2 pathway only for catabolism (Y in Fig. 6b). Experimentally, these combinations should be easy to identify because of the different product yields; in the first

**Table A.1**

Catabolic reactions of glucose for aerobic and fermentation pathways.  $\Delta_{cat}H_{glu}$  is the enthalpy change of catabolism and  $\gamma_{SOM}$  is the degree of reduction of SOM. Hydrogen can be balance by adding  $H_2O$  to the product side.

Metabolic pathway	Catabolism on glucose	$\Delta_{cat}H_{glu}$ (kJ C-mol <sup>-1</sup> S)	Source
<b>AE:</b> Aerobic catabolism of glucose	$CH_2O_{(glu)} + O_2 \rightarrow CO_2$	$\frac{\gamma_{glu}}{4} \Delta H_T$	(Thornton, 1917)
<b>F1:</b> Fermentation of glucose to ethanol	$CH_2O_{(glu)} \rightarrow \frac{\gamma_{glu}}{\gamma_{eth}} CH_3O_{0.5(eth)} + \left(1 - \frac{\gamma_{glu}}{\gamma_{eth}}\right) CO_2$	-16.7	(Forrest et al., 1961)
<b>F2:</b> Fermentation of glucose to lactic acid	$CH_2O_{(glu)} \rightarrow CH_2O_{(lac)}$	-18.33	(Forrest et al., 1961)
<b>SOM:</b> Aerobic catabolism of SOM	$C_{SOM} + \frac{\gamma_{SOM}}{4} O_2 \rightarrow CO_2$	$\frac{\gamma_{SOM}}{4} \Delta H_T$	(Thornton, 1917)

**Table A.2**

Alternative formulations for the anabolic reactions for microbial growth (von Stockar et al., 2008; Battley, 2009).  $\Delta_{ana}H_B$  is the enthalpy change of anabolism calculated using the degree of reduction balance.  $\gamma_{glu}$ ,  $\gamma_B$  and  $\gamma_{SOM}$  are the degrees of reduction of glucose, biomass and SOM. The elemental formula of microbial biomass ( $CH_{1.8}O_{0.5}N_{0.2}$ ) is from Roels (1980a).  $NH_3$  is assumed to be the source of nitrogen in biomass. Hydrogen can be balance by adding  $H_2O$  to either side.

Alternative formulations	Anabolism on glucose	$\Delta_{ana}H_B$ (kJ C-mol <sup>-1</sup> B)
Electron balance	$\frac{\gamma_B}{\gamma_{glu}} CH_2O_{(glu)} \rightarrow CH_{1.8}O_{0.5}N_{0.2} + \left(\frac{\gamma_B}{\gamma_{glu}} - 1\right) CO_2$	0
Carbon balance	$CH_2O_{(glu)} \rightarrow CH_{1.8}O_{0.5}N_{0.2} + \left(\frac{\gamma_B}{\gamma_{glu}} - 1\right) O_2$	$\frac{\gamma_{glu} - \gamma_B}{4} \Delta H_T$
Biomass from products of catabolism	$CO_2 \rightarrow CH_{1.8}O_{0.5}N_{0.2} + \frac{\gamma_B}{4} O_2$	$-\frac{\gamma_B}{4} \Delta H_T$

option  $Y_{lac,F2} = 0.34$  and  $Y_{eth,F1} = 0.33$ ; and in the second option  $Y_{lac,F2} = 0.5$  and  $Y_{eth,F1} = 0.28$  (calculated using Eqs. (12) and (13)). Similarly, a unique CUE value can be found for two different values of CR in Fig. 6c. Thus, complementing measurements of CR with measurements of the end products of substrate metabolism other than  $CO_2$ , such as organic acids and alcohols, it could be possible to identify the underlying metabolic pathways, and estimate CUE.

## 6. Conclusion

The calorespirometric ratio is defined as the ratio of heat dissipation rate to respiration rate. To interpret the observed variability of CR in soils, we formulated a modeling framework based on previously existing bioenergetic theories (Roels, 1980a; Hansen et al., 2004; Von Stockar et al., 2006). Specifically, we provide mass and energy balances by taking into account three metabolic pathways and the effect of priming. Our framework shows that combined aerobic and fermentation pathways for substrate metabolism can contribute to the observed variation in CR from soils. Further, it shows that the presence of fermentation pathways can alter the CR values depending upon their rates (i.e., the degrees of aerobicity and fermentation) and associated growth yields. We have also developed a generalized relation between CR, CUE, and the rates and growth yields of aerobic and fermentative metabolic pathways. This relation can be used to estimate CUE from measured values of CR for various active metabolic pathways and to explain the variability of CUE that cannot be explained on the basis of the C balance alone. Furthermore, we provide a theoretical basis on how to use CR to identify and quantify the priming effect. Lastly, we analyzed the variability of CR and CUE with substrate quality, finding (as in previous works) that CR increases with increasing degree of reduction of the substrate, and it increases (respectively decreases) with CUE when the degree of reduction of the substrate is higher (lower) than biomass.

To summarize, the following must be considered when interpreting CR data: (1) possibility of metabolic pathways other than aerobic

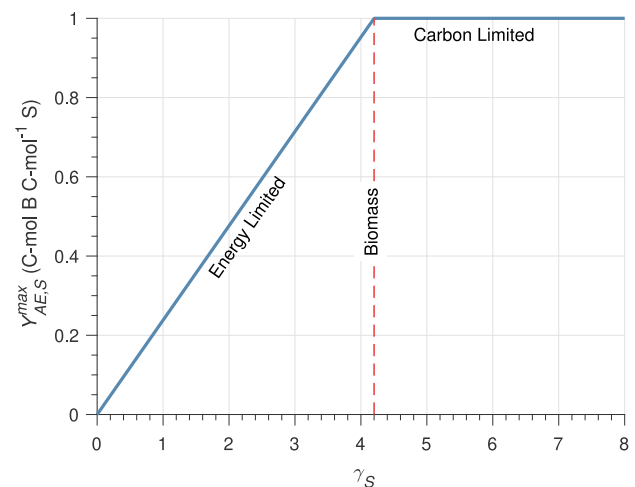


Fig. C.1. Thermodynamic limits on the aerobic growth yield ( $Y_{AE,S}^{max}$ ) as a function of the degree of reduction (DR =  $\gamma_S$ ) of the substrate. The vertical red line represents the DR of microbial biomass ( $\gamma_B = 4.2$ ).

growth by looking for common fermentation products such as ethanol or lactic acid; and identifying other electron acceptors that might favor anaerobic metabolism, (2) possibility that priming of SOM is significant, and (3) the non-uniqueness of CUE–CR relationship when using CR to estimate CUE. Therefore, we conclude that the calorespirometric ratio can emerge as a unifying metric containing information on both the energy and the mass fluxes exchanged by soil systems, but it requires complementary information on the dominant C flow pathways when used to estimate microbial CUE.

**Table A.3**

Aerobic growth yield ( $Y_{AE}$ ) compiled from [Smeaton and Van Cappellen \(2018\)](#) for various organic compounds and corresponding CR values calculated using Eq. (32) with a minor modification that  $\Delta_{AE}H_{glu}$  is replaced by the enthalpy of the growth reaction for a given substrate.

Substrate	Degree of reduction	Calorespirometric ratio (CR) (kJ/ C-mol CO <sub>2</sub> )	Growth yield ( $Y_{AE}$ ) (C-mol biomass C-mol <sup>-1</sup> S)	Catabolic product
glucose	4	423	0.66	CO <sub>2</sub>
glucose	4	449	0.46	CO <sub>2</sub>
glucose	4	436	0.48	acetate
glucose	4	432	0.51	acetate
glucose	4	443	0.42	acetate
lactic acid	4	435	0.32	acetate
lactic acid	4	417	0.42	acetate
lactic acid	4	423	0.39	acetate
ethanol	6	972	0.56	CO <sub>2</sub>
oxalate	1	80	0.09	CO <sub>2</sub>
oxalate	1	89	0.07	CO <sub>2</sub>
formate	2	139	0.27	CO <sub>2</sub>
formate	2	178	0.18	CO <sub>2</sub>
formate	2	196	0.13	CO <sub>2</sub>
formate	2	196	0.13	CO <sub>2</sub>
formate	2	185	0.16	CO <sub>2</sub>
formate	2	174	0.19	CO <sub>2</sub>
formate	2	153	0.24	CO <sub>2</sub>
formate	2	144	0.26	CO <sub>2</sub>

**Table A.4**

Calorespirometric ratio (CR) and carbon use efficiency (CUE) from different soils treatments amended with glucose, compiled from [Bölscher et al. \(2016\)](#).

Substrate	Soil treatment	CR (kJ C-mol <sup>-1</sup> CO <sub>2</sub> )	CUE (C-mol biomass C-mol <sup>-1</sup> S)
D-Glucose	Arable land	441	0.77
	Ley farming	398	0.73
	Grassland	377	0.75
	Forest	377	0.81
L-Alanine	Arable land	473	0.72
	Ley farming	586	0.72
	Grassland	639	0.72
	Forest	291	0.7
Glycogen	Arable land	523	0.86
	Ley farming	588	0.86
	Grassland	442	0.88
	Forest	318	0.88

**Table C.1**

Observed values of microbial growth yield ( $Y$  in C-mol bio/C-mol S), CO<sub>2</sub> yield ( $Y_C$  in C-mol CO<sub>2</sub>/C-mol S), product yield ( $Y_P$  in C-mol P/C-mol S), and heat yield ( $Y_Q$  in kJ/C-mol bio) data from [von Stockar and Birou \(1989\)](#).

	$Y$	$Y_C$	$Y_P$	$Y_Q$	CR (from data)	CR (our model)
(A) Fully aerobic ( $\alpha = 1$ )	0.57	0.41		328	458	438
(B) Complete fermentation ( $\alpha = 0$ )	0.13	0.28	0.5	119	54	49
(C) Mixed metabolism ( $\alpha = 0.5$ )	0.35	0.32	0.22	242	261	280

### CRedit authorship contribution statement

**Arjun Chakrawal:** Conceptualization, Methodology, Software, Writing - original draft. **Anke M. Herrmann:** Conceptualization, Writing - review & editing. **Hana Šantrůčková:** Writing - review & editing. **Stefano Manzoni:** Conceptualization, Supervision, Writing - review & editing, Funding acquisition.

### Declaration of competing interest

The authors declare that they have no known competing financial interests or personal relationships that could have appeared to influence the work reported in this paper.

### Acknowledgments

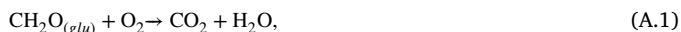
This research has been supported by the Vetenskapsrådet (grant no. 2016-04146) and Svenska Forskningsrådet Formas (grant no. 2017-00932). We thank the three anonymous reviewers whose comments/suggestions helped improve and clarify this manuscript.

### Appendix A. Derivation of the growth reactions

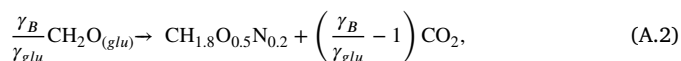
The microbial growth equation for each metabolic reaction (i.e. AE, F1 and F2) can be written by considering the sum of individual catabolic and anabolic reactions ([Battley, 1960b](#)). The chemical equations of each catabolic pathway for 1 C-mol of glucose and SOM are given in [Table A.1](#). The anabolic reaction can be expressed in three different ways ([von Stockar et al., 2008; Battley, 2009](#)). The first is based on metabolizing the substrate following an electron ( $e^-$ ) balance, the second is based on metabolizing the substrate following a carbon balance and, the third is based on the formation of biomass from the products of catabolism. These three options are described in [Table A.2](#). Details on how to write these alternative forms of anabolic reactions can be found elsewhere ([von Stockar et al., 2008; Battley, 2009](#)). We follow the first option for the anabolic reaction which is based on the assumption of equivalency of  $e^-$  availability in substrate and cell biomass (or product). Therefore,  $e^-$  acceptors are not involved and the enthalpy of the anabolic reaction is zero ([Table A.2](#)). A more detailed explanation of this argument can be found in [Battley \(2009\)](#).

and Kleerebezem and Van Loosdrecht (2010), and in the supplementary materials of Smeaton and Van Cappellen (2018).

It is worth noting that both catabolic and anabolic reactions are only a representation of complex biochemical reactions taking place within microbial cells. For example, catabolism of carbohydrates involves glycolysis, tricarboxylic acid cycle, and oxidative phosphorylation; however, when taking a systems perspective, all these processes are lumped, and we focus only on the input and output of the system. The growth equation is written for microorganisms growing on 1-C mol of substrate with specified growth efficiencies for each metabolic pathway. For example, the aerobic growth equation on glucose can be obtained by adding catabolic and anabolic reactions in such a way that results in the consumption of 1-C mole of glucose and production of  $Y_{AE}$  C-mol of biomass. The catabolic reaction of glucose in aerobic conditions is



and the corresponding anabolic reaction is

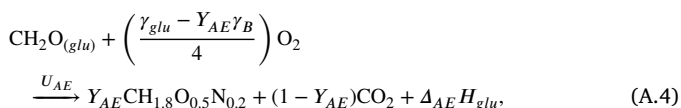


where the coefficient  $\frac{Y_B}{Y_{glu}}$  accounts for the lower DR of glucose compared to biomass. The enthalpy change of anabolism is calculated by writing the enthalpy balance of Eq. (A.2) using combustion enthalpy as reference,

$$\Delta_{ana}H_B = \frac{Y_B}{Y_{glu}} \Delta_C H_{glu} - \Delta_C H_B, \quad (\text{A.3})$$

where  $\Delta_C H_{glu}$  and  $\Delta_C H_B$  are the standard enthalpies of combustion of glucose and microbial biomass, respectively. Note that inserting the values  $\Delta_C H_{glu}$  and  $\Delta_C H_B$  using Thornton's rule (Eq. (B.1)) results in  $\Delta_{ana}H_B = 0$  irrespective of the type of substrate.

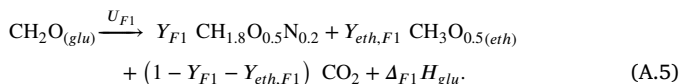
Because we aim to write the growth reaction for the consumption of 1 C-mol of glucose, we need to combine the catabolic and anabolic reactions and re-scale them accordingly. To do that, we multiply the catabolic (Eq. (A.1)) and anabolic (Eq. (A.2)) reactions by  $(1 - Y_{AE} \frac{Y_B}{Y_{glu}})$  and  $Y_{AE}$ , respectively, and sum them up to obtain the overall aerobic growth equation on glucose,



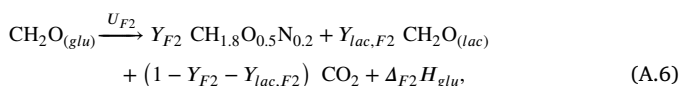
where  $Y_{AE}$ ,  $\Delta_{AE} H_{glu}$  and  $U_{AE} = \alpha U_{glu}$  are the growth yield, and enthalpy and rate of the reaction, respectively.

The microbial growth equations for the fermentation and SOM uptake pathways can be written in a similar way.

Fermentation of glucose to ethanol:



Fermentation of glucose to lactic acid:



where  $Y_{F1}$  and  $Y_{F2}$  are the growth yields in (C-mol biomass C-mol<sup>-1</sup> substrate);  $\Delta_{F1} H_{glu}$  and  $\Delta_{F2} H_{glu}$  are the enthalpies of reaction (kJ C-mol<sup>-1</sup> glu); and  $U_{F1} = \beta U_{glu}$  and  $U_{F2} = \lambda U_{glu}$  are the rates of the reactions in C-mol substrate/h for Eqs. (A.5) and (A.6), respectively.  $Y_{eth,F1}$  and  $Y_{lac,F2}$  can be calculated using the degree of reduction balance of Eq. (A.5) and (A.6), respectively,

$$Y_{eth,F1} = \frac{Y_{glu} - Y_{F1} Y_B}{Y_{eth}}, \quad (\text{A.7})$$

$$Y_{lac,F2} = \frac{Y_{glu} - Y_{F2} Y_B}{Y_{lac}}. \quad (\text{A.8})$$

## Appendix B. Thornton's rule

According to Thornton (1917), the enthalpy change during the aerobic mineralization of an organic compound can be approximately given by the moles of oxygen utilized in the complete combustion reaction multiplied by Thornton's coefficient ( $\Delta H_T$ ). We use the value of  $\Delta H_T = -455 \pm 15 \text{ kJ mol}^{-1} \text{ O}_2$  for a generic organic compound and  $-469 \text{ kJ mol}^{-1} \text{ O}_2$  for glucose. For a generic organic compound,  $C_S$ , with degree of reduction  $\gamma_S$ ; the enthalpy of combustion ( $\Delta_C H_S$ ) can be written as,

$$\Delta_C H_S = \frac{\gamma_S}{4} \Delta H_T \quad (\text{B.1})$$

where subscripts  $C$  and  $S$  in  $\Delta_C H_S$  refer to 'combustion' and 'organic substrate', respectively. A discussion on the limitations of Thornton's rule can be found in Wadsö and Hansen (2015). By convention,  $\Delta_C H_S$  is a negative quantity for exothermic reactions but for the purpose of estimating heat released, we consider only its magnitude.

## Appendix C. Thermodynamic limits to the growth yields

CUE is a function of both rates and yield values of individual metabolic growth pathways (Eq. (27)). The uptake rates are constrained by the kinetics of microbial growth; however, the maximum possible yields are constrained by thermodynamic principles (Von Stockar et al., 2006; Roels, 1980a). According to the second law of thermodynamics, growth yield is maximum when Gibbs energy obtained from catabolism is completely used by anabolism, leading to an equilibrium growth at infinitesimally slow rate (Von Stockar et al., 2006). A similar constraint based on the enthalpy of the growth reaction can be used; i.e., the maximum growth yield is theoretically achieved when the enthalpy of the growth reaction is zero, indicating that catabolism provides exactly the amount of enthalpy required by anabolism. Thus, setting the overall enthalpy change in Eq. (20) to zero, we obtain the maximum possible yield (here specifically for glucose metabolism),

$$Y_{i,glu}^{max} = \frac{\Delta_{cat,i} H_{glu}}{Y_{ana} \Delta_{cat,i} H_{glu} - \Delta_{ana} H_B}, \quad (\text{C.1})$$

where subscript  $i$  represents different glucose metabolic pathways, i.e., AE, F1, or F2. Since  $\Delta_{ana} H_B = 0$  (due to the selected formulation for the anabolic reaction, Appendix A), the maximum yield is found as,

$$Y_{i,glu}^{max} = \frac{1}{Y_{ana}} = \frac{Y_{glu}}{Y_B} = \frac{4}{4.2} = 0.95. \quad (\text{C.2})$$

Therefore, the maximum limits of  $Y_{AE}$ ,  $Y_{F1}$  and  $Y_{F2}$  are all equal to 0.95. It should be noted that for the fermentation pathways, the maximum yield values are theoretical maximum and in reality, these values are never achieved because at these theoretical maximum values the product yields ( $Y_{eth,F1}$  and  $Y_{lac,F2}$ ) would be zero, which is biochemically/biologically impossible. Using these maximum growth yields, we can calculate the maximum limit of CUE in the case of combined metabolism that is also equal to 0.95.

These enthalpy based thermodynamic limit for yield can be generalized to any substrate. For example, under aerobic growth conditions, the thermodynamically feasible range of yield  $Y_{AE,S}^{max}$  (subscript  $AE$  for aerobic and  $S$  for substrate) is calculated as a function of the degree of reduction of the substrate  $\gamma_S$  Heijnen and Roels (1981) as,

$$0 \leq Y_{AE,S}^{max} \leq \min \left( \frac{\gamma_S}{Y_B}, 1 \right) \quad (\text{C.3})$$

Fig. C.1 shows the theoretical limit of the growth yield for varying DR of organic substrates. Substrates with DR lower than biomass (e.g., glucose) are more oxidized than biomass, and substrates with DR higher than biomass (e.g., ethanol) are more reduced than biomass. The anabolism of 1 C-mol of biomass requires 1 C-mol of substrate based on carbon stoichiometry; however, 1 C-mol of a substrate with  $\gamma_S < \gamma_B$  does not have enough electrons needed in the anabolic

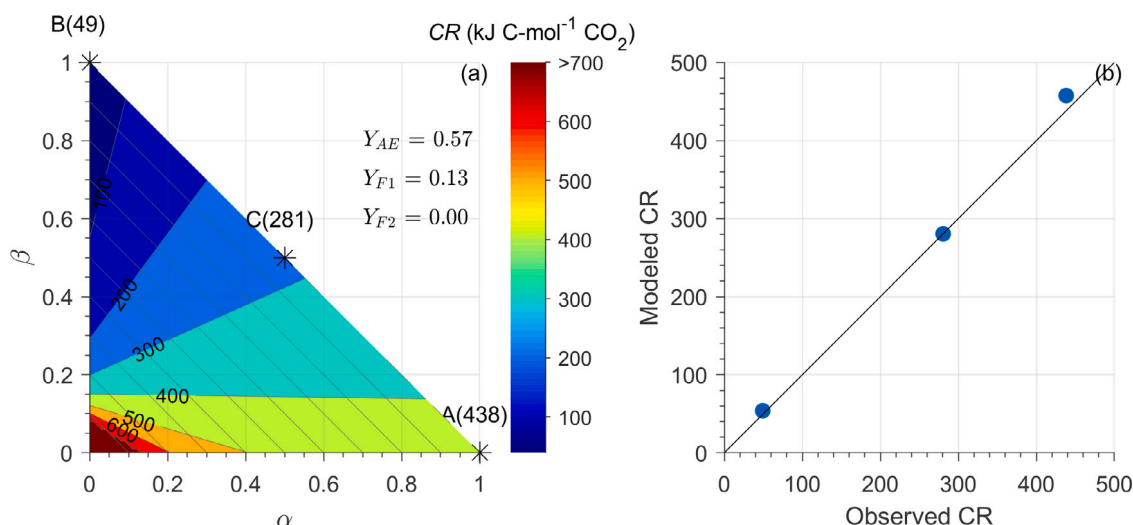


**Fig. C.2.** (a) Variation of CR as a function of fractional rates of aerobic (α) and fermentation pathways F1 (β) and F2 (λ) are shown under the combined aerobic + F1 growth conditions. Contour lines of CR are calculated from taking the growth yield values from Heijnen and Roels (1981). Experimentally observed values of CR recalculated from Heijnen and Roels (1981) are shown in parentheses at the star symbol. (b) Observed and modeled CR value against 1:1 line. Note that all three metabolic pathways are active but biomass is growing only if yield values are non zero.

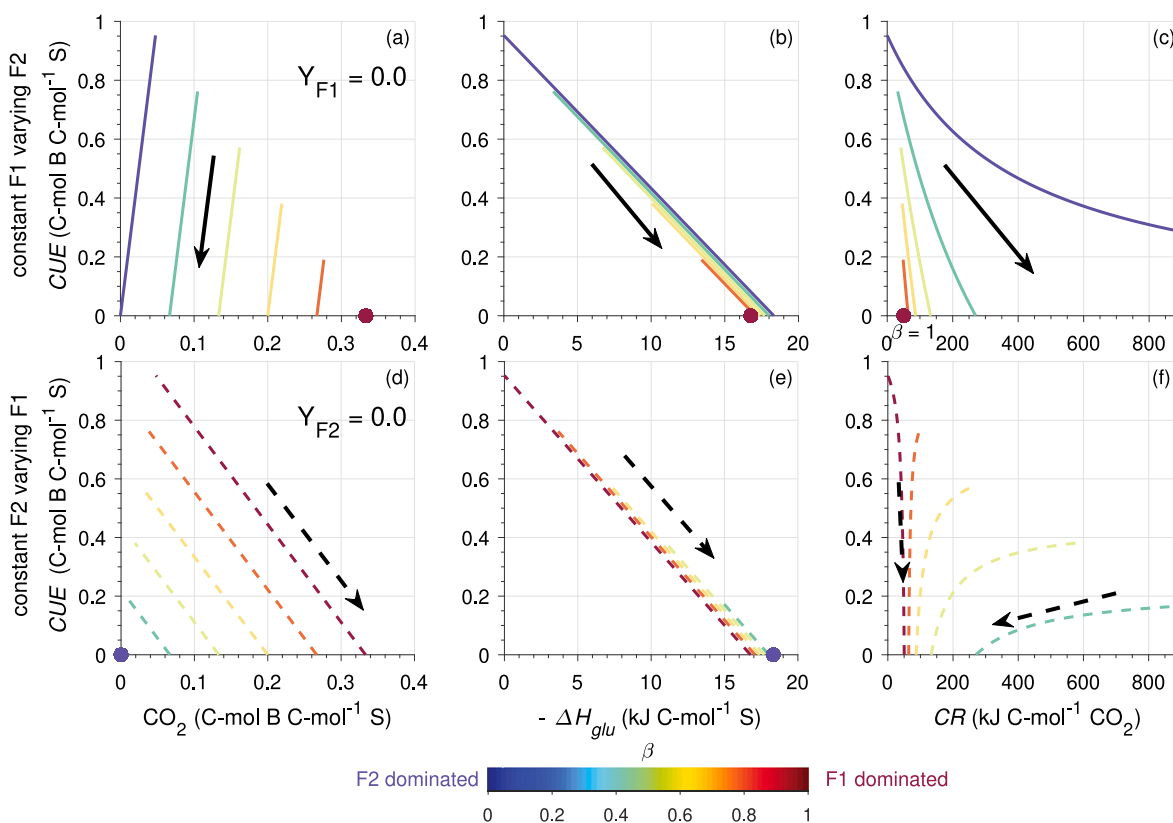


**Fig. D.1.** Scenario 2 Section 3.2.1 for Y<sub>F1</sub> and Y<sub>F2</sub> = 0: Variation of CUE with CO<sub>2</sub> yield (a and d), enthalpy dissipated as heat (b and e), and the CR (c and f) for varying degrees of β for AE, F1 and F2 pathways. In each panel, one of the growth yields (as indicated on the y-axis) is varied (decreasing) according to the arrow.

reaction. Therefore, growth is energy limited and the theoretical  $Y_{AE,S}^{max}$  can never approach 1. In contrast, 1 C-mol of substrate with  $\gamma_S > \gamma_B$  can provide more electrons that are needed by the anabolic reaction, so that anabolism is carbon limited because the number of carbon moles of biomass would be constrained by the number of carbon moles of substrate available. This leads to a theoretical yield of 1 for reduced substrates. However, it should be noted that this is a thermodynamic limit, and the actual growth yields on reduced substrates are less than 1 (Roels, 1980b) (see Fig. C.1).

### Appendix D. Variation of CUE with amount of CO<sub>2</sub>, heat, and CR for glucose metabolism

In this Appendix, we provide additional figures (Figs. D.1–D.3) showing the variation of CUE with the amount of CO<sub>2</sub> and heat released, and with CR, during uptake and metabolism of glucose via combinations of two fermentation pathways. These figures explain the contributions of CO<sub>2</sub> and heat exchanges to CR in scenario two in

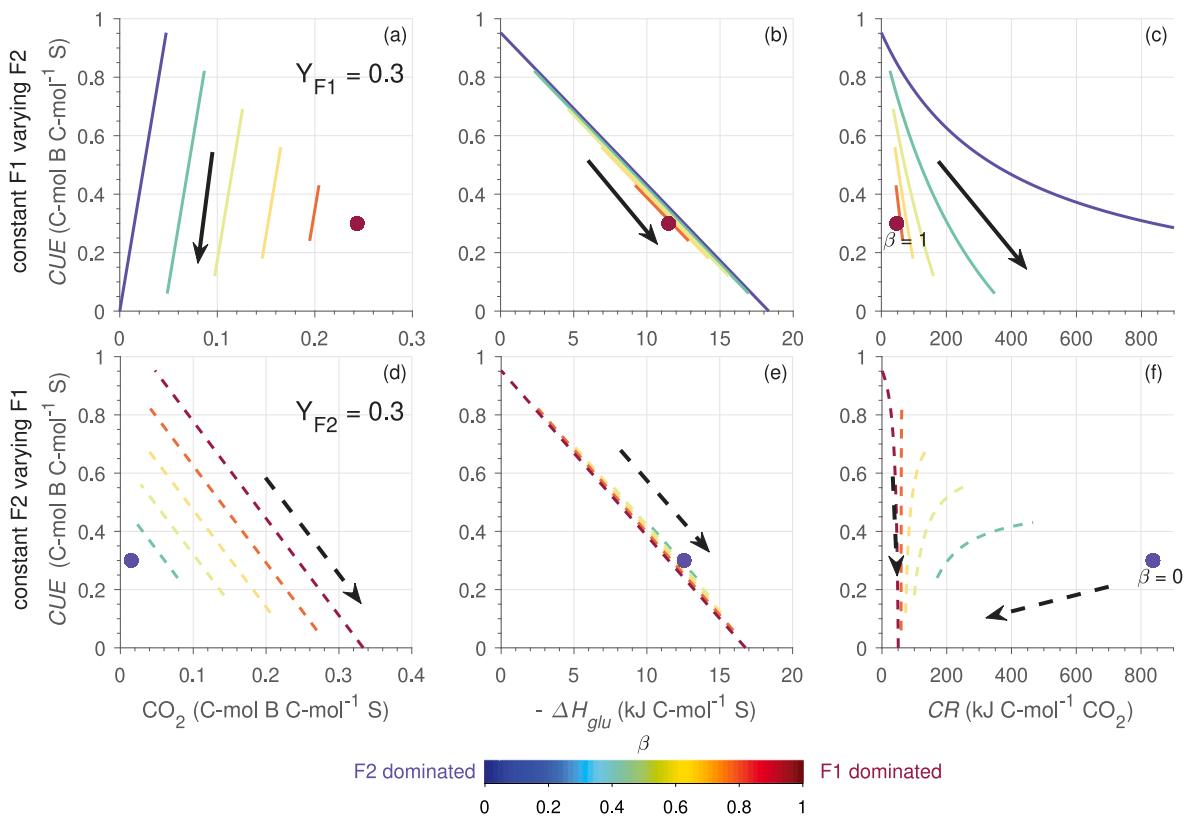


Fig. D.2. Scenario 2 Section 3.2.1 for  $Y_{F1}$  and  $Y_{F2} = 0.3$ : Variation of CUE with  $CO_2$  yield (a and d), enthalpy dissipated as heat (b and e), and the CR (c and f) for varying degrees of  $\beta$  for AE, F1 and F2 pathways. In each panel, one of the growth yields (as indicated on the y-axis) is varied (decreasing) according to the arrow.

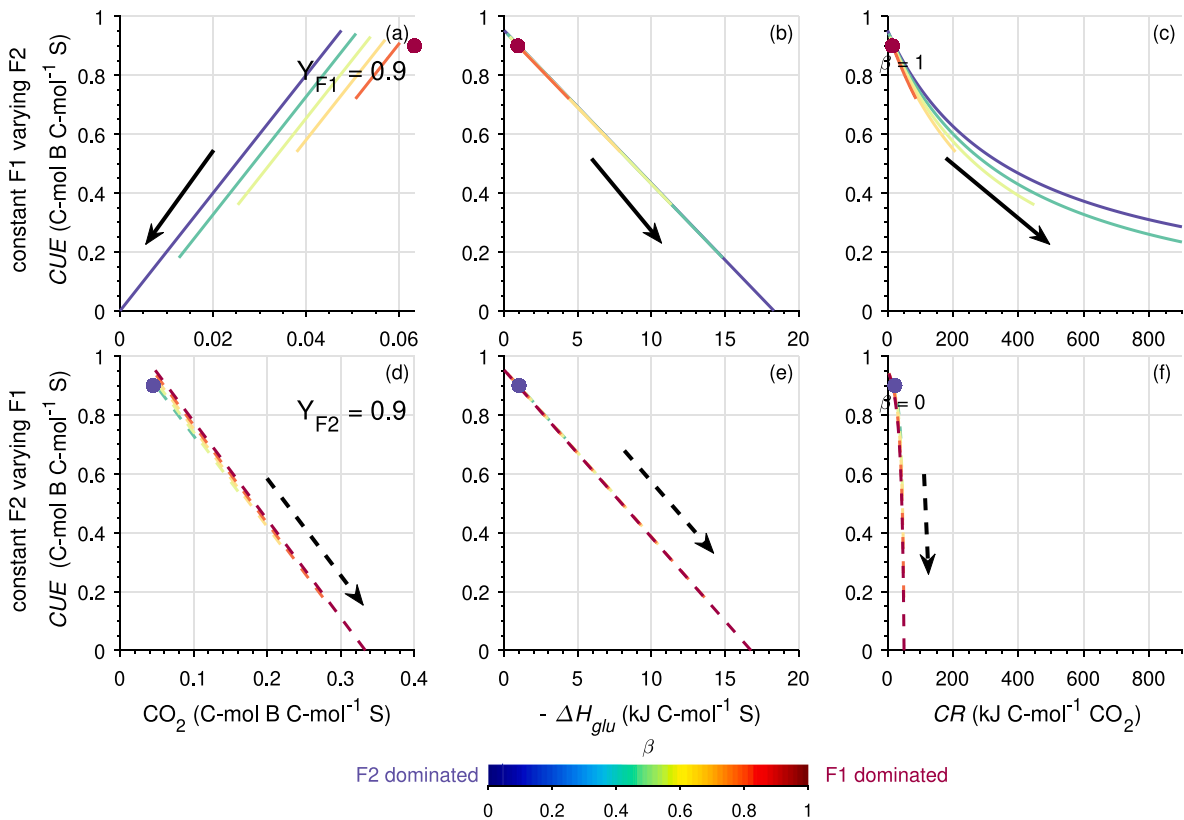


Fig. D.3. Scenario 2 Section 3.2.1 for  $Y_{F1}$  and  $Y_{F2} = 0.9$ : Variation of CUE with  $CO_2$  yield (a and d), enthalpy dissipated as heat (b and e), and the CR (c and f) for varying degrees of  $\beta$  for AE, F1 and F2 pathways. In each panel, one of the growth yields (as indicated on the y-axis) is varied (decreasing) according to the arrow.

Section 3.2.1 (i.e., Fig. 6b). CR effects on CUE depend on the chosen values of  $Y_{F1}$ ,  $Y_{F2}$ , and  $\beta$ , which are allowed to vary in Figs. D.1–D.3.

Fig. D.1 shows how CUE varies with  $\text{CO}_2$ , heat released, and CR, when the fractional rate  $\beta$  is increased from 0 (F2 only) to 1 (F1 only; lines with different color). In the top panels (solid lines), glucose is metabolized at a fixed  $Y_{F1} = 0$  and a variable F2 yield. Decreasing the F2 yield causes CUE and  $\text{CO}_2$  to also decrease, while heat release is increased. As a result, CUE decreases with increasing CR for any value of  $\beta$ . In the bottom panels (dashed lines)  $Y_{F2} = 0$  and F1 yield is variable. Here, decreasing F1 yield causes a decrease in CUE, while  $\text{CO}_2$  and heat release increase. As a result, CUE decreases with increasing CR only at high  $\beta$  values, and increases at low  $\beta$ . As  $\beta$  approaches zero ( $\gamma \rightarrow 1$ ), only the F2 pathway remains active, so that the solid lines in Fig. D.1c converge towards the dotted–dashed line in Fig. 6a; and the dashed lines in Fig. D.1f tend to infinity. Similarly, as  $\beta$  approaches one ( $\gamma \rightarrow 0$ ) and only the F1 pathway remains active, the solid lines in Fig. D.1c converge to the red dot (the value of CR without microbial growth), and the dashed lines in Fig. D.1f converge towards the dashed line in Fig. 6a. Unlike the first case (top panel), in the second case (bottom panel) CUE–CR is highly sensitive to the selected  $\beta$  and  $Y_{F2}$  values, and CUE–CR switches from a direct to an inverse relationship. Figs. D.2 and D.3 can be explained similar to Fig. D.1, but now the yields that are kept fixed are higher than zero.

## References

- Amenabar, M.J., Shock, E.L., Roden, E.E., Peters, J.W., Boyd, E.S., 2017. Microbial substrate preference dictated by energy demand rather than supply. *Nat. Geosci.* 10 (8), 577–581. <http://dx.doi.org/10.1038/NGEO2978>.
- Arcand, M.M., Levy-Booth, D.J., Helgason, B.L., 2017. Resource legacies of organic and conventional management differentiate soil microbial carbon use. *Front. Microbiol.* 8, <http://dx.doi.org/10.3389/fmicb.2017.02293>.
- Arnholdt-Schmitt, B., 2017. Respiration traits as novel markers for plant robustness under the threat of climate change: A Protocol for validation. In: Jagadis Gupta, K. (Ed.), *Plant Respiration and Internal Oxygen: Methods and Protocols*. Springer New York, New York, NY, pp. 183–191.
- Arnholdt-Schmitt, B., Hansen, L.D., Nogales, A., 2016. Calorespirometry, oxygen isotope analysis and functional-marker-assisted selection (“CalOxy-FMAS”) for genotype screening: A novel concept and tool kit for predicting stable plant growth performance and functional marker identification. *Brief. Funct. Genomics* 15 (1), 10–15.
- Barja, I., Núñez, L., 1999. Microcalorimetric measurements of the influence of glucose concentration on microbial activity in soils. *Soil Biol. Biochem.* 31 (3), 441–447. [http://dx.doi.org/10.1016/S0038-0717\(98\)00149-7](http://dx.doi.org/10.1016/S0038-0717(98)00149-7).
- Barros, N., Feijóo, S., Hansen, L.D., 2011. Calorimetric determination of metabolic heat,  $\text{CO}_2$  rates and the calorespirometric ratio of soil basal metabolism. *Geoderma* 160 (3), 542–547. <http://dx.doi.org/10.1016/j.geoderma.2010.11.002>.
- Barros, N., Hansen, L.D., Piñeiro, V., Pérez-Cruzado, C., Villanueva, M., Proupín, J., Rodríguez-Añón, J.A., 2016a. Factors influencing the calorespirometric ratios of soil microbial metabolism. *Soil Biol. Biochem.* 92, 221–229. <http://dx.doi.org/10.1016/j.soilbio.2015.10.007>.
- Barros, N., Hansen, L.D., Piñeiro, V., Vikegard, P., 2016b. Calorimetry measures the response of soil organic matter biodegradation to increasing temperature. *J. Therm. Anal. Calorim.* 123 (3), 2397–2403. <http://dx.doi.org/10.1007/s10973-015-4947-8>.
- Barros, N., Salgado, J., Rodríguez-Añón, J.A., Proupín, J., Villanueva, M., Hansen, L.D., 2010. Calorimetric approach to metabolic carbon conversion efficiency in soils: Comparison of experimental and theoretical models. *J. Therm. Anal. Calorim.* 99 (3), 771–777. <http://dx.doi.org/10.1007/s10973-010-0673-4>.
- Barros Pena, N., 2018. Calorimetry and soil biodegradation: Experimental procedures and thermodynamic models. In: Bidoia, E.D., Montagnoli, R.N. (Eds.), *Toxicity and Biodegradation Testing*. In: *Methods in Pharmacology and Toxicology*, Springer New York, New York, NY, pp. 123–145. [http://dx.doi.org/10.1007/978-1-4939-7425-2\\_7](http://dx.doi.org/10.1007/978-1-4939-7425-2_7).
- Battley, E.H., 1960a. A theoretical approach to the study of the thermodynamics of growth of *saccharomyces cerevisiae* (Hansen). *Physiol. Plant.* 13 (4), 674–686. <http://dx.doi.org/10.1111/j.1399-3054.1960.tb08090.x>.
- Battley, E.H., 1960b. Enthalpy changes accompanying the growth of *saccharomyces cerevisiae* (Hansen). *Physiol. Plant.* 13 (4), 628–640. <http://dx.doi.org/10.1111/j.1399-3054.1960.tb08085.x>.
- Battley, E.H., 2009. Is electron equivalence between substrate and product preferable to C-mol equivalence in representations of microbial anabolism applicable to “origin of life” environmental conditions? *J. Theoret. Biol.* 260 (2), 267–275. <http://dx.doi.org/10.1016/j.jtbi.2009.05.032>.
- Battley, E.H., 2013. A theoretical study of the thermodynamics of microbial growth using *saccharomyces cerevisiae* and a different free energy equation. *Q. Rev. Biol.* 88 (2), 69–96. <http://dx.doi.org/10.1086/670529>.
- Birou, B., Marison, I.W., Stockar, U.V., 1987. Calorimetric investigation of aerobic fermentations. *Biotechnol. Bioeng.* 30 (5), 650–660. <http://dx.doi.org/10.1002/bit.260300509>.
- Bölscher, T., Ågren, G.I., Herrmann, A.M., 2020. Land-use alters the temperature response of microbial carbon-use efficiency in soils – a consumption-based approach. *Soil Biol. Biochem.* 140, 107639. <http://dx.doi.org/10.1016/j.soilbio.2019.107639>.
- Bölscher, T., Paterson, E., Freitag, T., Thornton, B., Herrmann, A.M., 2017. Temperature sensitivity of substrate-use efficiency can result from altered microbial physiology without change to community composition. *Soil Biol. Biochem.* 109, 59–69. <http://dx.doi.org/10.1016/j.soilbio.2017.02.005>.
- Bölscher, T., Wadsö, L., Börjesson, G., Herrmann, A.M., 2016. Differences in substrate use efficiency: Impacts of microbial community composition, land use management, and substrate complexity. *Biol. Fertil. Soils* 52 (4), 547–559. <http://dx.doi.org/10.1007/s00374-016-1097-5>.
- Boye, K., Herrmann, A.M., Schaefer, M.V., Tfaily, M.M., Fendorf, S., 2018. Discerning microbially mediated processes during redox transitions in flooded soils using carbon and energy balances. *Front. Environ. Sci.* 6 (May), <http://dx.doi.org/10.3389/fenvs.2018.00015>.
- Boye, K., Noël, V., Tfaily, M.M., Bone, S.E., Williams, K.H., Bargar, J.R., Fendorf, S., 2017. Thermodynamically controlled preservation of organic carbon in floodplains. *Nat. Geosci.* 10 (6), 415–419. <http://dx.doi.org/10.1038/ngeo2940>.
- Chaires, J.B., Hansen, L.D., Keller, S., Brautigam, C.A., Zhao, H., Schuck, P., 2015. Biocalorimetry. *Methods* 76, 1–2. <http://dx.doi.org/10.1016/j.ymeth.2015.02.001>.
- Colombi, T., Herrmann, A.M., Vallenback, P., Keller, T., 2019. Cortical cell diameter is key to energy costs of root growth in wheat. *Plant Physiol.* 180 (4), 2049–2060. <http://dx.doi.org/10.1104/pp.19.00262>, URL: <http://www.plantphysiol.org/content/180/4/2049>.
- Cotrufio, M.F., Wallenstein, M.D., Boot, C.M., Denef, K., Paul, E., 2013. The microbial efficiency-matrix stabilization (MEMS) framework integrates plant litter decomposition with soil organic matter stabilization: Do labile plant inputs form stable soil organic matter? *Global Change Biol.* 19 (4), 988–995. <http://dx.doi.org/10.1111/gcb.12113>.
- Erickson, L., 1987. Energy requirements in biological systems. In: *Thermal and Energetic Studies of Cellular Biological Systems*. Elsevier, pp. 14–33. <http://dx.doi.org/10.1016/B978-0-7236-0909-4.50006-1>.
- Forrest, W.W., Walker, D.J., Hopgood, M.F., 1961. Enthalpy changes associated with the lactic fermentation of glucose. *J. Bacteriol.* 82 (5), 685–690.
- Geyer, K.M., Dijkstra, P., Sinsabaugh, R., Frey, S.D., 2019. Clarifying the interpretation of carbon use efficiency in soil through methods comparison. *Soil Biol. Biochem.* 128, 79–88. <http://dx.doi.org/10.1016/j.soilbio.2018.09.036>.
- Geyer, K.M., Kyker-Snowman, E., Grandy, A.S., Frey, S.D., 2016. Microbial carbon use efficiency: Accounting for population, community, and ecosystem-scale controls over the fate of metabolized organic matter. *Biogeochemistry* 127 (2), 173–188. <http://dx.doi.org/10.1007/s10533-016-0191-y>.
- Gnaiger, E., Kemp, R.B., 1990. Anaerobic metabolism in aerobic mammalian cells: Information from the ratio of calorimetric heat flux and respirometric oxygen flux. *Biochim. Biophys. Acta (BBA) - Bioenergetics* 1016 (3), 328–332. [http://dx.doi.org/10.1016/0005-2728\(90\)90164-Y](http://dx.doi.org/10.1016/0005-2728(90)90164-Y).
- Gommers, P.J.F., van Schie, B.J., van Dijken, J.P., Kuenen, J.G., 1988. Biochemical limits to microbial growth yields: An analysis of mixed substrate utilization. *Biotechnol. Bioeng.* 32 (1), 86–94. <http://dx.doi.org/10.1002/bit.260320112>.
- Hansen, L.D., MacFarlane, C., McKinnon, N., Smith, B.N., Criddle, R.S., 2004. Use of calorespirometric ratios, heat per  $\text{CO}_2$  and heat per O<sub>2</sub>, to quantify metabolic paths and energetics of growing cells. *Thermochim. Acta* 422 (1–2), 55–61. <http://dx.doi.org/10.1016/j.tca.2004.05.033>.
- Heijnen, J.J., Roels, J.A., 1981. A macroscopic model describing yield and maintenance relationships in aerobic fermentation processes. *Biotechnol. Bioeng.* 23 (4), 739–763. <http://dx.doi.org/10.1002/bit.260230407>.
- Herrmann, A.M., Bölscher, T., 2015. Simultaneous screening of microbial energetics and  $\text{CO}_2$  respiration in soil samples from different ecosystems. *Soil Biol. Biochem.* 83, 88–92. <http://dx.doi.org/10.1016/j.soilbio.2015.01.020>.
- Herrmann, A.M., Colombi, T., 2019. Energy use efficiency of root growth – a theoretical bioenergetics framework. *Plant Signal. Behav.* 14 (12), 1685147. <http://dx.doi.org/10.1080/15592324.2019.1685147>.
- Herrmann, A.M., Coucheney, E., Nunan, N., 2014. Isothermal microcalorimetry provides new insight into terrestrial carbon cycling. *Environ. Sci. Technol.* 48 (8), 4344–4352. <http://dx.doi.org/10.1021/es403941h>.
- Keiluweit, M., Wanzek, T., Kleber, M., Nico, P., Fendorf, S., 2017. Anaerobic microsites have an unaccounted role in soil carbon stabilization. *Nature Commun.* 8 (1), 1771. <http://dx.doi.org/10.1038/s41467-017-01406-6>.
- Kleerebezem, R., Van Loosdrecht, M.C., 2010. A generalized method for thermodynamic state analysis of environmental systems. *Crit. Rev. Environ. Sci. Technol.* 40 (1), 1–54. <http://dx.doi.org/10.1080/10643380802000974>.
- Kuzuyakov, Y., 2010. Priming effects: Interactions between living and dead organic matter. *Soil Biol. Biochem.* 42 (9), 1363–1371. <http://dx.doi.org/10.1016/j.soilbio.2010.04.003>.

- la Cecilia, D., Riley, W.J., Maggi, F., 2019. Biochemical modeling of microbial memory effects and catabolite repression on soil organic carbon compounds. *Soil Biol. Biochem.* 128, 1–12. <http://dx.doi.org/10.1016/j.soilbio.2018.10.003>.
- Leak, D.J., Dalton, H., 1986. Growth yields of methanotrophs. *Appl. Microbiol. Biotechnol.* 23 (6), 470–476. <http://dx.doi.org/10.1007/BF02346062>.
- Ljungholm, K., Norén, B., Wadsö, I., 1979. Microcalorimetric observations of microbial activity in normal and acidified soils. *Oikos* 33 (1), 24–30. <http://dx.doi.org/10.2307/3544507>.
- Manzoni, S., Čapek, P., Mooshammer, M., Lindahl, B.D., Richter, A., Šantrůčková, H., 2017. Optimal metabolic regulation along resource stoichiometry gradients. *Ecol. Lett.* 20 (9), 1182–1191. <http://dx.doi.org/10.1111/ele.12815>.
- Manzoni, S., Čapek, P., Porada, P., Thurner, M., Winterdahl, M., Beer, C., Bruchert, V., Frouz, J., Herrmann, A.M., Lindahl, B.D., Lyon, S.W., Santruckova, H., Vico, G., Way, D., 2018. Reviews and syntheses : Carbon use efficiency from organisms to ecosystems - definitions, theories, and empirical evidence. *Biogeosciences* 15 (19), 5929–5949.
- Manzoni, S., Taylor, P., Richter, A., Porporato, A., Ågren, G.I., 2012. Environmental and stoichiometric controls on microbial carbon-use efficiency in soils. *New Phytol.* 196 (1), 79–91. <http://dx.doi.org/10.1111/j.1469-8137.2012.04225.x>.
- Maskow, T., Paufler, S., 2015. What does calorimetry and thermodynamics of living cells tell us? *Methods* 76, 3–10. <http://dx.doi.org/10.1016/j.ymeth.2014.10.035>.
- Maskow, T., Rothe, A., Jakob, T., Paufler, S., Wilhelm, C., 2019. Photocalorespirometry (photo-CR): A novel method for access to photosynthetic energy conversion efficiency. *Sci. Rep.* 9 (1), 1–13. <http://dx.doi.org/10.1038/s41598-019-45296-8>.
- Matheson, S., Ellingson, D.J., McCarlie, V.W., Smith, B.N., Criddle, R.S., Rodier, L., Hansen, L.D., 2004. Determination of growth and maintenance coefficients by calorimetry. *Funct. Plant Biol.* 31 (9), 929. <http://dx.doi.org/10.1071/FP03029>.
- Minkevich, I.G., Eroshin, V.K., 1973. Productivity and heat generation of fermentation under oxygen limitation. *Folia Microbiol.* 18 (5), 376–385. <http://dx.doi.org/10.1007/BF02875932>.
- Monod, J., 1949. The growth of bacterial cultures. *Annu. Rev. Microbiol.* 3 (1), 371–394. <http://dx.doi.org/10.1146/annurev.mi.03.100149.002103>.
- Moyano, F.E., Manzoni, S., Chenu, C., 2013. Responses of soil heterotrophic respiration to moisture availability: An exploration of processes and models. *Soil Biol. Biochem.* 59, 72–85. <http://dx.doi.org/10.1016/j.soilbio.2013.01.002>.
- Nagai, S., 1979. Mass and energy balances for microbial growth kinetics. In: *Advances in Biochemical Engineering*, vol. 11. pp. 49–83.
- Roels, J.A., 1980a. Application of macroscopic principles to microbial metabolism. *Biotechnol. Bioeng.* 22 (12), 2457–2514. <http://dx.doi.org/10.1002/bit.260221202>.
- Roels, J., 1980b. Simple model for the energetics of growth on substrates with different degrees of reduction. *Biotechnol. Bioeng.* 22 (1), 33–53. <http://dx.doi.org/10.1002/bit.260220104>.
- Roels, J., 1983. *Energetics and Kinetics in Biotechnology*. Elsevier Biomedical Press.
- Rutgers, M., van der Gulden, H.M.L., Dam, K., 1989. Thermodynamic efficiency of bacterial growth calculated from growth yield of *Pseudomonas oxalaticus* OX1 in the chemostat. *Biochim. Biophys. Acta (BBA) - Bioenergetics* 973 (2), 302–307. [http://dx.doi.org/10.1016/S0005-2728\(89\)80436-0](http://dx.doi.org/10.1016/S0005-2728(89)80436-0).
- Smeaton, C.M., Van Cappellen, P., 2018. Gibbs energy dynamic yield method (GEDYM): Predicting microbial growth yields under energy-limiting conditions. *Geochim. Cosmochim. Acta* 241, 1–16. <http://dx.doi.org/10.1016/j.gca.2018.08.023>.
- Sparling, G.P., 1983. Estimation of microbial biomass and activity in soil using microcalorimetry. *J. Soil Sci.* 34 (2), 381–390. <http://dx.doi.org/10.1111/j.1365-2389.1983.tb01043.x>.
- Spohn, M., Klaus, K., Wanek, W., Richter, A., 2016. Microbial carbon use efficiency and biomass turnover times depending on soil depth – implications for carbon cycling. *Soil Biol. Biochem.* 96, 74–81. <http://dx.doi.org/10.1016/j.soilbio.2016.01.016>.
- Thornton, W., 1917. XV. the relation of oxygen to the heat of combustion of organic compounds. *London Edinburgh Dublin Philos. Mag. J. Sci.* 33 (194), 196–203.
- Tijhuis, L., Van Loosdrecht, M.C., Heijnen, J.J., 1993. A thermodynamically based correlation for maintenance gibbs energy requirements in aerobic and anaerobic chemotrophic growth. *Biotechnol. Bioeng.* 42 (4), 509–519. <http://dx.doi.org/10.1002/bit.260420415>.
- von Stockar, U., Birou, B., 1989. The heat generated by yeast cultures with a mixed metabolism in the transition between respiration and fermentation. *Biotechnol. Bioeng.* 34 (1), 86–101. <http://dx.doi.org/10.1002/bit.260340112>.
- von Stockar, U., Liu, J.S., 1999. Does microbial life always feed on negative entropy? thermodynamic analysis of microbial growth. *Biochim. Biophys. Acta (BBA) - Bioenergetics* 1412 (3), 191–211. [http://dx.doi.org/10.1016/S0005-2728\(99\)00065-1](http://dx.doi.org/10.1016/S0005-2728(99)00065-1).
- von Stockar, U., Marison, I.W., 1989. The use of calorimetry in biotechnology. In: *Reinventing Higher Education: The Promise of Innovation*. Springer, Berlin, Heidelberg, pp. 93–136. <http://dx.doi.org/10.1007/BFb0009829>.
- Von Stockar, U., Maskow, T., Liu, J., Marison, I.W., Patiño, R., 2006. Thermodynamics of microbial growth and metabolism: an analysis of the current situation. *J. Biotechnol.* 121 (4), 517–533. <http://dx.doi.org/10.1016/j.jbiotec.2005.08.012>.
- von Stockar, U., van der Wielen, L.A., 2013. *Biothermodynamics: The Role of Thermodynamics in Biochemical Engineering*. EPFL Press.
- von Stockar, U., Vojinović, V., Maskow, T., Liu, J., 2008. Can microbial growth yield be estimated using simple thermodynamic analogies to technical processes? *Biothermodynamics, Chemical Engineering and Processing: Process Intensification Biothermodynamics*, 47 (6), 980–990. <http://dx.doi.org/10.1016/j.cep.2007.02.016>.
- Wadsö, L., Hansen, L.D., 2015. Calorespirometry of terrestrial organisms and ecosystems. *Methods* 76, 11–19. <http://dx.doi.org/10.1016/j.ymeth.2014.10.024>.
- Westerhoff, H.V., Lolkema, J.S., Otto, R., Hellingwerf, K.J., 1982. Thermodynamics of growth non-equilibrium thermodynamics of bacterial growth the phenomenological and the mosaic approach. *Biochim. Biophys. Acta (BBA) - Rev. Bioenergetics* 683 (3), 181–220. [http://dx.doi.org/10.1016/0304-4173\(82\)90001-5](http://dx.doi.org/10.1016/0304-4173(82)90001-5).
- Wutzler, T., Reichstein, M., 2013. Priming and substrate quality interactions in soil organic matter models. *Biogeosciences* 10 (3), 2089–2103. <http://dx.doi.org/10.5194/bg-10-2089-2013>.